

# Integrable boundary interaction in 3D target space: the “pillow-brane” model

Sergei L. Lukyanov and Alexander B. Zamolodchikov

NHETC, Department of Physics and Astronomy  
Rutgers University, Piscataway, NJ 08855-0849, USA

and

L.D. Landau Institute for Theoretical Physics  
Chernogolovka, 142432, Russia

## Abstract

We propose a model of boundary interaction, with three-dimensional target space, and the boundary values of the field  $\mathbf{X} \in \mathbb{R}^3$  constrained to lay on a two-dimensional surface of the “pillow” shape. We argue that the model is integrable, and suggest that its exact solution is described in terms of certain linear ordinary differential equation.

---

August 2012

# 1 Introduction

A class of quantum field theories in 2D space-time, in which conformal invariance is broken only by boundary conditions, is of interest both in connection with “brane” states in string theories [1], and as useful models of quantum Brownian motion [2]. Among such theories are the “brane models”, where the bulk CFT consists of a collection of  $N$  free massless scalar fields  $\mathbf{X}(z, \bar{z})$ , associated with the coordinates of  $N$ -dimensional “target space”, while the interaction is introduced through nonlinear constraints imposed at the boundary of 2D “world sheet”: The boundary values  $\mathbf{X}_B$  are required to lay on a nonlinear hypersurface  $\Sigma \subset \mathbb{R}^N$  - the “brane”.<sup>1</sup>

Interaction generated by such constraints requires renormalization, and therefore in general the shape of the hypersurface  $\Sigma$  “flows” under the Renormalization Group (RG) transformations. In the weak coupling regime such RG flow reduces to an interesting case of geometric flow - the so called mean curvature flow (for review, see [3]) - in the same way as the Ricci flow [4, 5] emerges as the weak-coupling limit of the bulk RG flow of 2D sigma models [6]. When the curvature of  $\Sigma$  is not small (on the scale set by the size of the quantum fluctuations of the gradients  $\partial\mathbf{X}$ ), the brane models require non-perturbative treatment. Approach beyond the perturbation theory exists if the model is *integrable*. This means that the boundary constraint is consistent with infinitely many commuting integrals of motion of the world-sheet theory. Integrable models of this kind, with two-dimensional target space, and with  $\Sigma$  being certain curves in  $\mathbb{R}^2$ , were previously studied in Refs. [7, 8]. In this work we extend analysis to three-dimensional target space, and study a model in which  $\Sigma$  is a special surface in  $\mathbb{R}^3$ , of the topology of  $S^2$  and a shape resembling a good quality pillow. After a good nap, we found it comfortable enough to be named the pillow-brane.<sup>2</sup>

As in [7, 8], we will consider the simplest nontrivial setting, in which the bulk CFT lives inside the disk  $|z| < R$  ( $(z, \bar{z})$  are standard complex coordinates in 2D Euclidean space-time) and the non-conformal interaction takes place at the boundary  $|z| = R$ . The bulk CFT involves three-component scalar field  $\mathbf{X} = (X, Y, Z) \in \mathbb{R}^3$ , and apart from the boundary constraint (see below), the model is described by the Euclidean action

$$\mathcal{A} = \frac{1}{4\pi} \int_{|z| < R} d^2z \partial_a \mathbf{X} \cdot \partial_a \mathbf{X} + \mathcal{A}_B, \quad (1.1)$$

which includes the so-called  $B$ -field term

$$\mathcal{A}_B = -\frac{i}{4\pi} \int_{|z| < R} d^2z \varepsilon^{ab} \mathbf{B}(\mathbf{X}) \cdot (\partial_a \mathbf{X} \times \partial_b \mathbf{X}), \quad (1.2)$$

The boundary interaction is introduced mainly through the boundary constraint

$$\mathbf{X}_B \equiv \mathbf{X}|_{|z|=R} \in \Sigma^2, \quad (1.3)$$

where  $\Sigma^2$  is certain surface in  $\mathbb{R}^3$ , of the shape described in detail below. We assume the field  $\mathbf{B}$  to be solenoidal,<sup>3</sup> i.e.,

$$\nabla \cdot \mathbf{B} = 0, \quad (1.4)$$

---

<sup>1</sup>Here we use the term “brane” in reference to a generic boundary constraint of this kind. Of course, on-shell stringy brane states are associated only with conformally invariant boundary conditions [1].

<sup>2</sup>The pillow can be regarded as deformed sphere. Integrability of the spherical-brane model, with  $\Sigma = S^2 \subset \mathbb{R}^3$ , was previously discussed in Ref. [7].

<sup>3</sup>Otherwise the nonlinear term (1.2) would break conformal invariance in the bulk.

so that the last term in (1.1) is in fact a part of the boundary interaction

$$\mathcal{A}_B = -\frac{i}{2\pi} \oint_{|z|=R} d\tau \mathbf{A}(\mathbf{X}_B) \cdot \mathbf{e}_j \partial_\tau \eta^j, \quad (1.5)$$

where  $\mathbf{A}(\mathbf{X})$  is the vector potential,

$$\mathbf{B} = \nabla \times \mathbf{A}. \quad (1.6)$$

Here  $\tau$  is a parameter along the boundary  $|z| = R$ ,  $\eta^j = (\eta^1, \eta^2)$  are some local coordinates on  $\Sigma^2$ , and

$$\mathbf{e}_j = \frac{\partial \mathbf{X}_B}{\partial \eta^j}. \quad (1.7)$$

are two tangent vectors to  $\Sigma^2$ .

As was already mentioned, generally the shape  $\mathbf{X}_B = \mathbf{X}_B(\eta_1, \eta_2)$  of the surface  $\Sigma^2$  “flows” with the RG parameter  $t$  (defined here as  $t = -\log(E)$  in terms of the normalization energy scale  $E$ ). The RG flow equations can be derived perturbatively, within the loop expansion, which applies in the limit when the curvature of the brane is small. The one-loop equations can be taken from Ref. [9]. For our model (1.1) they read

$$\mathbf{n} \cdot \dot{\mathbf{X}}_B - \frac{K}{1 + B_n^2} = 0, \quad (1.8)$$

and

$$\frac{1}{\sqrt{g}} \frac{\partial}{\partial \eta^i} (\sqrt{g} g^{ij} D_j) = 0, \quad (1.9)$$

where

$$D_j = (\mathbf{n} \cdot \dot{\mathbf{X}}_B) B_j + \frac{1}{1 + B_n^2} \frac{\partial B_n}{\partial \eta^j}. \quad (1.10)$$

In these equations dot signifies derivative with respect to the RG parameter  $t$ ,  $K$  stands for is the mean (external) curvature of  $\Sigma^2$ ,  $g_{ij} = \mathbf{e}_i \cdot \mathbf{e}_j$  is the induced metric,  $g = \det(g_{ij})$ ,  $B_n = \mathbf{B} \cdot \mathbf{n}$  denotes the normal component of the field  $\mathbf{B}$ , and  $B_j = \mathbf{B} \cdot \mathbf{e}_j$ .

In Section 2 we show that with a suitable choice of the *pure imaginary* field  $\mathbf{B}$  (see Eqs.(2.9), (2.10) below) the RG flow equations are satisfied by the following scale-dependent surface:

$$\sqrt{(1 + w_1)(1 + w_2)} \cos\left(\frac{Z_B}{\sqrt{n+2}}\right) = \sqrt{w_1 w_2} \cosh\left(\frac{X_B}{\sqrt{n\nu}}\right) + \cosh\left(\frac{Y_B}{\sqrt{n(1-\nu)}}\right). \quad (1.11)$$

Here  $n > 0$  and  $0 < \nu < 1$  are real parameters which are independent on the RG energy scale, while  $w_{1,2} = w_{1,2}(E)$  “flow” with the scale. They are given by two distinct real solutions of the equation

$$\kappa^2 = w^{a_1} (1 + w)^{a_3} (a_2(2 + a_2) w^2 - 2a_1 a_2 w + a_1(2 + a_1)), \quad (1.12)$$

where

$$a_1 = n\nu, \quad a_2 = n(1 - \nu), \quad a_3 = -n - 2, \quad (1.13)$$

and  $\kappa$  is inversely proportional to  $E$ ,  $\kappa = \frac{E_*}{E}$ . The proportionality coefficient  $E_*$  (the integration constant of the RG flow equation) sets the “physical scale” for the model: physical quantities (like the overlap amplitudes (1.22) below) will depend on the dimensionless combination  $E_*R$ . In what follows we always take the normalization scale  $E$  equal to  $R^{-1}$ , so that  $\kappa$  in the left-hand side of (1.12) coincides with this combination,

$$\kappa = E_*R. \quad (1.14)$$

Eq.(1.12) then relates the coefficients  $w_{1,2}$  in (1.11) to the radius  $R$ . The shape of the surface (1.11) is sketched in Fig.1, from which the origin of the term “pillow-brane” should be evident.

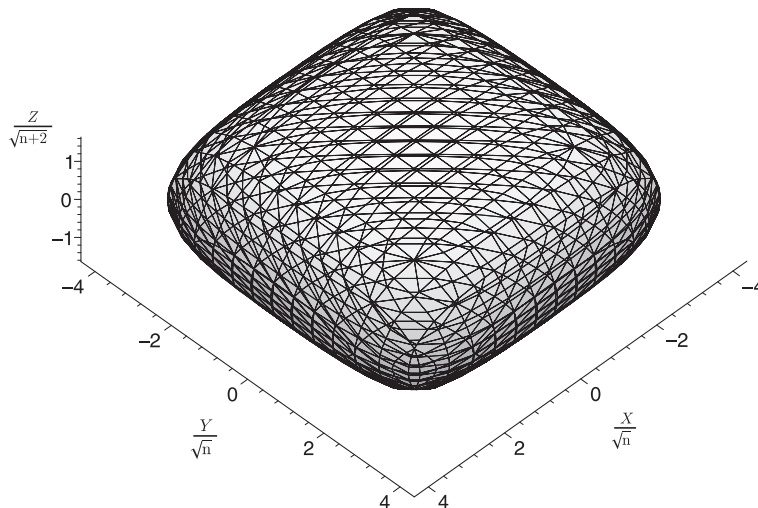


Figure 1: The surface (1.11) with  $n = 20$ ,  $\nu = \frac{1}{2}$  and  $\kappa^{\frac{2}{n}} = 0.01$ . Its pillow-like shape gives the name to the model.

Strictly speaking, the one-loop approximation applies only in the limit  $n \rightarrow \infty$ , in which the curvature  $K$  of the surface (1.11) becomes uniformly small. In this limit it is superfluous to distinguish between  $n$  and  $n+2$ , as we do in writing Eqs.(1.11), (1.12). However, we believe (and will argue below) that the shape described by these equations is “perturbatively exact”, i.e., Eqs.(1.11), (1.12) satisfy the RG flow equations to all orders in the loop expansion. In this connection let us note two symmetries of Eqs.(1.11),(1.12). One is the interchange between  $X$  and  $Y$ , or, more precisely, the transformation

$$X \leftrightarrow Y, \quad Z \rightarrow Z; \quad a_1 \leftrightarrow a_2, \quad a_3 \rightarrow a_3; \quad w \leftrightarrow w^{-1}. \quad (1.15)$$

The other symmetry is formally similar,

$$\begin{aligned} X \leftrightarrow Z, \quad Y \rightarrow Y; \quad a_1 \leftrightarrow a_3, \quad a_2 \rightarrow a_2; \quad w \leftrightarrow -(1+w), \\ \kappa^2 \rightarrow (-1)^{a_2} \kappa^2, \end{aligned} \quad (1.16)$$

but more subtle, in that it exchanges  $n \leftrightarrow -(n+2)$  and therefore in effect interchanges  $X$  with imaginary  $Z$  in (1.11).

The general “pillow” solution (1.11), (1.12) has several interesting limiting cases. Thus, when  $\nu \rightarrow 0$  and  $w_1 \rightarrow 0$ , the pillow degenerates into the noncompact cylindrical surface  $\Sigma^2 \rightarrow \mathbb{R} \otimes \Sigma^1$ , where the one-dimensional curve  $\Sigma^1$  has a “paperclip” shape. That is, in this limit the first component of the

field  $\mathbf{X}$  decouples, and the remaining boundary QFT reduces to the paperclip-brane model of Ref. [8]. Another shape can be obtained from (1.11), (1.12) by taking the limit  $\nu \rightarrow 0$ ,  $n \rightarrow \infty$ ,  $w_{1,2} \rightarrow 0$ , while keeping the parameters  $\lambda = n\nu$ ,  $v_{1,2} = w_{1,2}/\nu$  and  $\bar{\kappa}^2 = \kappa^2 \nu^{-\lambda} \lambda^{-2}$  fixed. In this case the pillow becomes the surface of revolution (see Fig.2):

$$\frac{Y_B^2 + Z_B^2}{\lambda} = v_1 + v_2 - 2\sqrt{v_1 v_2} \cosh\left(\frac{X_B}{\sqrt{\lambda}}\right), \quad (1.17)$$

where  $v_{1,2}$  are two real solutions of the equation:

$$\bar{\kappa}^2 = v^\lambda e^{-\lambda v} \left( (1-v)^2 + \frac{2}{\lambda} \right). \quad (1.18)$$

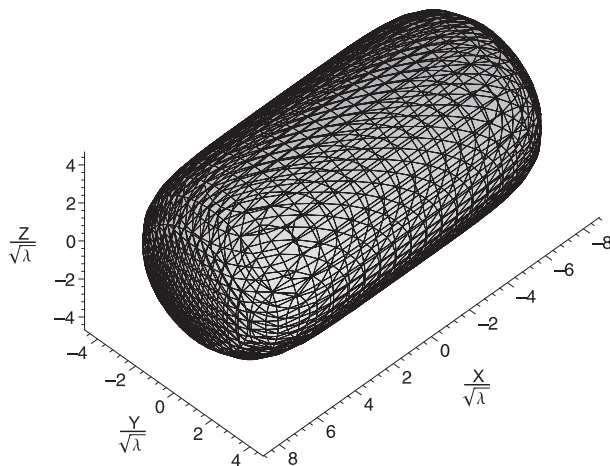


Figure 2: The  $U(1)$ -invariant limit (1.17) of the pillow surface, drawn with  $\bar{\kappa}^{\frac{2}{\lambda}} = 10^{-6}$ .

Finally, taking the limit  $\lambda \rightarrow \infty$ , the  $U(1)$ -invariant brane (1.17) turns to a sphere. Indeed, if  $\tilde{\kappa}^2 = \bar{\kappa}^2 \lambda e^\lambda$  is fixed, then  $v_{1,2} = 1 \pm \frac{1}{\sqrt{g\lambda}} + O(\lambda^{-1})$ , where  $g > 0$  solves the equation,

$$\tilde{\kappa} = \sqrt{\frac{1+2g}{g}} e^{-\frac{1}{4g}}, \quad (1.19)$$

and Eq.(1.18) reduces to

$$X_B^2 + Y_B^2 + Z_B^2 = \frac{1}{g}. \quad (1.20)$$

The sphere (1.19), (1.20) solves the RG flow equation with  $\mathbf{B} = 0$ . Some properties of this “spherical-brane” model was previously discussed in Ref. [7].

As was already mentioned, the pillow surface (1.11),(1.12) provides useful description only at  $n \gg 1$ , for otherwise the mean curvature at the round corners of the pillow surface in Fig.1 is not small, and non-perturbative effects may be significant. Moreover, even with large  $n$ , the perturbative treatment is limited to sufficiently short length scales, such that  $\kappa^{\frac{2}{n}} \ll 1$ . The large length scale behavior, where  $\kappa \gg 1$ , requires non-perturbative approach. In the main body of this paper we will propose full non-perturbative description of the pillow-brane model, valid at all scales and at all  $n > 0$ . The description will be given in terms of the boundary state. The boundary state  $|B\rangle$  associated

with certain boundary conditions is a special vector in the space of states  $\mathcal{H}$  of radial quantization of the bulk theory, in our case

$$\mathcal{H} = \int_{\mathbf{P}} \mathcal{F}_{\mathbf{P}} \otimes \bar{\mathcal{F}}_{\mathbf{P}}, \quad (1.21)$$

where  $\mathcal{F}_{\mathbf{P}}$  is the Fock space of three-component right-moving boson with the zero-mode momentum  $\mathbf{P} = (P_1, P_2, P_3)$ . The notion of the boundary state is explained in [10, 11] (see also [8]), and we will not do it here. We just mention that its overlap with the Fock vacuum  $|\mathbf{P}\rangle$  is related in a simple way to the un-normalized one-point function of the exponential field inserted at the center of the disk,

$$\langle e^{i\mathbf{P}\cdot\mathbf{X}}(0,0) \rangle_{\text{disk}} = R^{1/2-\mathbf{P}^2/2} \langle \mathbf{P} | B \rangle. \quad (1.22)$$

This overlap amplitude  $\langle \mathbf{P} | B \rangle$ , which we sometimes call the partition function, is the main object of our interest in this paper. When the boundary condition is not conformally invariant, the amplitude depend on the scale parameter (1.14), and we will use the notation

$$\langle \mathbf{P} | B \rangle = Z(\mathbf{P} | \kappa). \quad (1.23)$$

In this paper we describe some basic properties of the partition function (1.23) of the pillow brane model, and argue that this boundary interaction is integrable. The meaning of this statement is explained in Section 5. Finally, we propose exact expression for the partition function, Eq.(6.7), in terms of solutions of linear ordinary differential equation (6.1), (6.2), test it against various expansions in the pillow-brane model, and find remarkable agreement.

## 2 Solution of one-loop RG equations

In this section, to simplify the notation we will omit the subscript  $B$  in the notation for the boundary values  $\mathbf{X}_B$ , writing simply  $(X, Y, Z)$  for  $(X_B, Y_B, Z_B)$ .

Let us use the pair of Cartesian coordinates  $(X, Y)$  as local coordinates on the brane  $\Sigma^2$  and write  $\mathbf{B} = (B_X, B_Y, B_Z)$ . Then the first RG flow equation (1.8) becomes:

$$L^2 \dot{Z} = Z_{xx}(1 + Z_y^2) + Z_{yy}(1 + Z_x^2) - 2 Z_x Z_y Z_{xy}, \quad (2.1)$$

with

$$L^2 = 1 + Z_x^2 + Z_y^2 + (B_Z - Z_x B_X - Z_y B_Y)^2. \quad (2.2)$$

Here subscripts  $x$  and  $y$  signifies the partial derivatives with respect to the coordinates  $X$  and  $Y$ , respectively. One can check that the ansatz

$$\cos\left(\frac{Z}{\sqrt{n}}\right) = a(t) \cosh\left(\frac{X}{\sqrt{n\nu}}\right) + b(t) \cosh\left(\frac{Y}{\sqrt{n(1-\nu)}}\right), \quad (2.3)$$

and

$$L = \frac{\ell(t)}{\left|\sin\left(\frac{Z}{\sqrt{n}}\right)\right|}, \quad (2.4)$$

with  $n$  and  $\nu$  being arbitrary constants, satisfies Eq.(2.1), provided the parameters  $a(t), b(t)$  and  $\ell(t)$ , are functions of the RG “time”  $t$  which satisfy the following system of ordinary differential equations:

$$\begin{aligned}\ell^2(t) \nu(1-\nu) n \dot{a} &= a \left( (1-\nu)(1-a^2) - (1+\nu)b^2 \right), \\ \ell^2(t) \nu(1-\nu) n \dot{b} &= b \left( \nu(1-b^2) + (\nu-2)a^2 \right).\end{aligned}\quad (2.5)$$

We further specialize the ansatz (2.4) by imposing an additional condition

$$\ell^2(t) = 1 - \frac{a^2}{\nu} - \frac{b^2}{1-\nu}.\quad (2.6)$$

With this, the form of the normal component of the  $\mathbf{B}$ -field is simplified significantly. Combining Eqs.(2.2)-(2.4) and (2.6) one obtains,

$$B_Z - Z_x B_X - Z_y B_Y = i \frac{(1-\nu) a \cosh\left(\frac{X}{\sqrt{n\nu}}\right) - \nu b \cosh\left(\frac{Y}{\sqrt{n(1-\nu)}}\right)}{\sqrt{\nu(1-\nu)} \sin\left(\frac{Z}{\sqrt{n}}\right)}.\quad (2.7)$$

Let us turn back on the RG flow equations (1.9). It would certainly be satisfied if one set  $D_j = 0$ , or, equivalently

$$B_j = -\frac{1}{K} \frac{\partial B_n}{\partial \eta^j}.\quad (2.8)$$

This determines the tangential components of the field  $\mathbf{B}$  and, with (2.7), completely specifies the vector  $\mathbf{B}$  at each point of the surface (2.3),

$$\begin{aligned}B_X|_{\Sigma} &= -i \frac{a((1-\nu)^2 - b^2) \sinh\left(\frac{X}{\sqrt{n\nu}}\right)}{\sqrt{1-\nu} Q}, \\ B_Y|_{\Sigma} &= i \frac{b(\nu^2 - a^2) \sinh\left(\frac{Y}{\sqrt{n(1-\nu)}}\right)}{\sqrt{\nu} Q}, \\ B_Z|_{\Sigma} &= i \frac{(b^2\nu^2 - a^2(1-\nu)^2) \sin\left(\frac{Z}{\sqrt{n}}\right)}{\sqrt{(1-\nu)\nu} Q},\end{aligned}\quad (2.9)$$

where

$$\begin{aligned}Q &= a \left( (1-\nu)(a^2 - 1) + b^2(1+\nu) \right) \cosh\left(\frac{X}{\sqrt{n\nu}}\right) + \\ & b \left( \nu(b^2 - 1) + a^2(2-\nu) \right) \cosh\left(\frac{Y}{\sqrt{n(1-\nu)}}\right).\end{aligned}\quad (2.10)$$

At any given RG “time”  $t$ , Eqs.(2.9) define the field  $\mathbf{B}$  at all points of the surface  $\Sigma = \Sigma(t)$ , Eq.(2.3). However, since the surface itself flows with  $t$ , these equations in fact give the field  $\mathbf{B}$  in certain part of the bulk of  $\mathbb{R}^3$ , the part which is swept by  $\Sigma(t)$  in the course of the RG evolution. For this, one has to regard the components (2.9) as the functions of non-linear coordinates  $(X, Y, t)$ , with  $Z$  related to these variables through (2.3). It is not difficult to verify that in this domain Eqs.(2.9) indeed define a vector which satisfies (1.4). It is straightforward to obtain

$$\nabla \cdot \mathbf{B} = \frac{\partial}{\partial X} (\dot{Z} B_X) + \frac{\partial}{\partial Y} (\dot{Z} B_Y) + \frac{\partial}{\partial t} (B_Z - Z_x B_X - Z_y B_Y).\quad (2.11)$$

Eq.(2.10) can be written in the form

$$Q = \ell^2(t) \sqrt{n} \nu(1 - \nu) \dot{Z} \sin\left(\frac{Z}{\sqrt{n}}\right),$$

and then the condition  $\nabla \cdot \mathbf{B} = 0$  follows from (2.11).

Finally, one has to solve the system of ordinary differential equations (2.5) and (2.6). Here we will restrict our attention to the case  $n > 0$ ,  $0 < \nu < 1$ , and look for positive solutions  $a, b > 0$ , such that

$$a, b \rightarrow 0, \quad \text{as } t \rightarrow -\infty. \quad (2.12)$$

Geometrically, these conditions single out compact surface (2.3), with topology of a sphere and a pillow shape shown in Fig. 1, which grows in the  $X$  and  $Y$  directions in the ultraviolet limit  $t \rightarrow -\infty$ . It is convenient to replace the positive  $a$  and  $b$  by parameters  $w_{1,2}$  defined through the equations

$$a = \sqrt{\frac{w_1 w_2}{(1 + w_1)(1 + w_2)}}, \quad b = \frac{1}{\sqrt{(1 + w_1)(1 + w_2)}}. \quad (2.13)$$

We will assume that both  $w_1$  and  $w_2$  are real, and  $w_2 > w_1$ , so the condition (2.12) can be equivalently written in the form

$$w_1 \rightarrow 0, \quad w_2 \rightarrow +\infty, \quad \text{as } t \rightarrow -\infty. \quad (2.14)$$

One can check that both functions  $w_1(t)$  and  $w_2(t)$  satisfy the same differential equation:

$$n \dot{w} \left( \frac{1}{1 + w} - \frac{\nu}{w} \right) + 2 = 0, \quad (2.15)$$

and hence

$$e^{\frac{2}{n}(t-t_{1,2})} = \frac{w_{1,2}^\nu}{1 + w_{1,2}}, \quad (2.16)$$

were  $t_1$  and  $t_2$  are the integration constants. To clarify the meaning of the RG invariants  $t_{1,2}$ , we first write them as

$$t_1 = t_* - \frac{\mu}{2}, \quad t_2 = t_* + \frac{\mu}{2}. \quad (2.17)$$

Then  $t_*$  can be identify with the logarithm of the physical scale  $E_*$  of the model, while  $\mu$  represents a non trivial first integral of the system (2.5), (2.6). It admits the following representation in terms of the original coefficients  $a$  and  $b$ ,

$$e^{\frac{2\mu}{n}} = \frac{1 + b^2 - a^2 + \sqrt{((a-b)^2 - 1)((a+b)^2 - 1)}}{1 + b^2 - a^2 - \sqrt{((a-b)^2 - 1)((a+b)^2 - 1)}} \times \left[ \frac{1 - a^2 - b^2 - \sqrt{((a-b)^2 - 1)((a+b)^2 - 1)}}{1 - a^2 - b^2 + \sqrt{((a-b)^2 - 1)((a+b)^2 - 1)}} \right]^\nu. \quad (2.18)$$

One can show that up to a simple factor, the RG invariant  $\mu$  coincides with a total flux of the field  $\mathbf{B}$  (2.9) through the pillow surface,

$$\mu = \frac{1}{4\pi i} \oint_{\text{pillow}} d\eta_1 \wedge d\eta_2 \sqrt{g} B_n. \quad (2.19)$$



Strictly speaking, presence of a nonzero flux (2.19) contradicts our assumption about the solenoidal form of the field  $\mathbf{B}$ , Eq.(1.6), and for this reason in this work we will consider only solutions with

$$\mu = 0 . \tag{2.20}$$

However, we do not think that this is the last word about the flux  $\mu$  in the brane models of this type. It is plausible that generalizations of the pillow-brane model to the case of nonzero flux is possible, and we hope to return to this question in the future.

Once (2.20) is assumed, the parameters  $w_1$  and  $w_2$  in (2.13) become two real solutions of the same equation

$$\kappa^{\frac{2}{n}} = \frac{w^\nu}{1+w} , \tag{2.21}$$

where  $\log(\kappa) = t - t_*$ . Note that this equation is the one-loop approximation to (1.12), which reduces to (2.21) in the limit  $n \rightarrow \infty$ . We believe that (1.12) incorporates all higher-loop corrections.

### 3 Semiclassical analysis of the pillow-brane model

The one-point function (1.22) admits representation in terms of the functional integral,

$$\langle e^{i\mathbf{P}\cdot\mathbf{X}}(0,0) \rangle_{\text{disk}} = \int \mathcal{D}X \mathcal{D}Y \mathcal{D}Z e^{iP_1 X + iP_2 Y + iP_3 Z}(0,0) e^{-\mathcal{A}[X,Y,Z]} , \tag{3.1}$$

where  $\mathbf{P} = (P_1, P_2, P_3)$ , and the integration is over the fields  $X(z, \bar{z})$ ,  $Y(z, \bar{z})$  and  $Z(z, \bar{z})$ , subjects to the constraint (1.11) at the boundary  $|z| = R$ . It will be useful to regard the components  $P_j$  of the zero mode momentum  $\mathbf{P}$  as complex variables. Since the pillow surface is compact, the integrand (3.1) is bounded for any complex vectors  $\mathbf{P}$ , hence the overlap  $\langle \mathbf{P} | B \rangle$  in Eq.(1.22) is an entire function of its components. When  $P_j$  are taken to be pure imaginary, these parameters can be interpreted as external fields coupled to the boundary values  $\mathbf{X}_B = (X_B, Y_B, Z_B)$ . One makes a shift

$$\mathbf{X} \rightarrow \mathbf{X} + i\mathbf{P} \log \frac{|z|}{R} , \tag{3.2}$$

of the integration variables in (3.1), bringing it to the form

$$\langle e^{i\mathbf{P}\cdot\mathbf{X}}(0,0) \rangle_{\text{disk}} = R^{-\mathbf{P}^2/2} \int \mathcal{D}\mathbf{X} e^{-\mathcal{A}[\mathbf{X}] - \mathcal{B}[\mathbf{X}_B]} , \tag{3.3}$$

where

$$\mathcal{B}[\mathbf{X}_B] = - \oint_{|z|=R} \frac{dz}{2\pi z} (P_1 X_B + P_2 Y_B + P_3 Z_B)(z) . \tag{3.4}$$

The representation (3.3) is most useful in the semiclassical limit. The semiclassical approximation is valid when the curvature of the pillow surface (1.11) is uniformly small. For this, one needs to have  $n \gg 1$  and also sufficiently small  $\kappa$ , such that  $\kappa^{\frac{1}{n}} \lesssim 1$ . Note that according to (1.12) one has to have sufficiently small  $R$  in order to meet the last condition. Therefore, semiclassical regime in the pillow-brane model corresponds to large  $n$  and sufficiently small length scales. In the leading semiclassical approximation the contribution in the path integral is dominated by the classical solutions minimizing  $\mathcal{A}[\mathbf{X}] + \mathcal{B}[\mathbf{X}_B]$ .

Let us first assume that the parameters  $P_j$  are small, so that the effect of the boundary term (3.4) saddle-point configurations is negligible. We write

$$(P_1, P_2, P_3) = \frac{2}{\sqrt{n}} \left( \frac{\alpha}{\sqrt{\nu}}, \frac{\beta}{\sqrt{1-\nu}}, \gamma \right) \quad (3.5)$$

and assume that  $\alpha, \beta, \gamma$  remain finite in the limit  $n \rightarrow \infty$ . The action  $\mathcal{A}[\mathbf{X}]$  is minimized by trivial classical solutions - the constant fields  $\mathbf{X}(z, \bar{z}) = \mathbf{X}_0$ , where  $\mathbf{X}_0 = (X_0, Y_0, Z_0)$  is any point on the pillow surface (1.11). The classical limit of (1.23) can be written as the integral

$$Z_{\text{class}} = \iint_{\text{pillow}} d\mathcal{M}(\mathbf{X}_0) e^{2i \left( \frac{\alpha X_0}{\sqrt{n\nu}} + \frac{\beta Y_0}{\sqrt{n(1-\nu)}} + \frac{\gamma Z_0}{\sqrt{n}} \right)}, \quad (3.6)$$

The integration measure  $d\mathcal{M}(\mathbf{X}_0)$  is determined by integrating out Gaussian fluctuations around the classical solution. In the presence of the  $B$ -field the measure was calculated in Ref. [12]. Up to the constant factor it has the Dirac-Born-Infeld form

$$d\mathcal{M} = g_D^3 \sqrt{g(1 + B_n^2)} \frac{d\eta_1 \wedge d\eta_2}{(2\pi)^2}, \quad (3.7)$$

where  $g_D = 2^{-\frac{1}{4}}$  is the boundary degeneracy associated with the Dirichlet conformal boundary condition.<sup>4</sup> In addition, the Gaussian fluctuations give rise to the one-loop term in the renormalization of the parameters  $w_1, w_2$  in (1.11), as is described by Eq.(2.21).

Using  $(X, Y)$  as local coordinates on the pillow surface, the measure (3.7) can be written as

$$d\mathcal{M}(\mathbf{X}_0) = g_D^3 \frac{\ell(t)}{(2\pi)^2} \frac{dX_0 \wedge dY_0}{\left| \sin \left( \frac{Z_0}{\sqrt{n}} \right) \right|}, \quad (3.8)$$

where  $\ell(t)$  is given by (2.6) and (2.13). Therefore the semiclassical partition function (3.6) admits the following representation

$$Z_{\text{class}} = \frac{n g_D^3}{2\pi} \sqrt{(\nu - (1-\nu)w_1)((1-\nu)w_2 - \nu)} \mathcal{I}(\alpha, \beta, \gamma), \quad (3.9)$$

where

$$\mathcal{I}(\alpha, \beta, \gamma) = \frac{1}{2\pi} \int_{-\infty}^{\infty} dx \int_{-\infty}^{\infty} dy \int_{-\frac{\pi}{2}}^{\frac{\pi}{2}} dz e^{2i(\alpha x + \beta y + \gamma z)} \times \delta(\sqrt{w_1 w_2} \cosh x + \cosh y - \sqrt{(1+w_1)(1+w_2)} \cos z). \quad (3.10)$$

The integral in (3.10) is calculated in closed form, in terms of the hypergeometric function,

$$\mathcal{I}(\alpha, \beta, \gamma) = \frac{Q_{-\alpha, \beta, \gamma}(w_2) Q_{\alpha, \beta, \gamma}(w_1) - Q_{\alpha, \beta, \gamma}(w_2) Q_{-\alpha, \beta, \gamma}(w_1)}{2i \alpha \sqrt{(1+w_1)(1+w_2)}}, \quad (3.11)$$

where

$$Q_{\alpha, \beta, \gamma}(w) = w^{-i\alpha} (1+w)^{\frac{1}{2}-\gamma} \times {}_2F_1\left(\frac{1}{2} - i\alpha + i\beta - \gamma, \frac{1}{2} - i\alpha - i\beta - \gamma, 1 - 2i\alpha; -w\right). \quad (3.12)$$

---

<sup>4</sup>The definition is as follows:  $g_D = \langle P | B_D \rangle$ , where  $|B_D\rangle$  is the boundary state of *uncompactified* boson  $X$  with the Dirichlet boundary condition  $X_B = 0$ , and the primary states  $|P\rangle$  are delta-normalized,  $\langle P | P' \rangle = \delta(P - P')$ .

Alternative form of (3.9) is obtained by transforming to the hypergeometric functions of the argument  $w^{-1}$ ,

$$Z_{\text{class}} = \sum_{\varepsilon, \varepsilon' = \pm 1} B_{\text{class}}(\varepsilon \alpha, \varepsilon' \beta, \varepsilon \varepsilon' \gamma) F_{\text{class}}(\varepsilon \alpha, \varepsilon' \beta, \varepsilon \varepsilon' \gamma | \kappa), \quad (3.13)$$

where

$$B_{\text{class}}(\alpha, \beta, \gamma) = \frac{n g_D^3}{2\pi} \frac{\sqrt{\nu(1-\nu)} w_1^{i\alpha} w_2^{-i\beta} \Gamma(-2i\alpha) \Gamma(-2i\beta)}{\Gamma(\frac{1}{2} - i\alpha - i\beta - \gamma) \Gamma(\frac{1}{2} - i\alpha - i\beta + \gamma)} \quad (3.14)$$

and

$$F_{\text{class}}(\alpha, \beta, \gamma | \kappa) = \sqrt{\frac{(\nu - (1-\nu)w_1)((1-\nu)w_2 - \nu)}{\nu(1-\nu)(1+w_1)(1+w_2)}} \times w_1^{-i\alpha} w_2^{i\beta} Q_{-\alpha, \beta, \gamma}(w_1) Q_{-\beta, \alpha, \gamma}(w_2^{-1}). \quad (3.15)$$

Advantage of this representation is that it makes explicit the singular behavior of  $Z_{\text{class}}$  at short scales  $\kappa \rightarrow 0$ , since in this limit we have

$$w_1 \sim \kappa^{\frac{2}{n\nu}} \rightarrow 0, \quad w_2 \sim \kappa^{-\frac{2}{n(1-\nu)}} \rightarrow \infty. \quad (3.16)$$

The above result was derived under the assumption that the zero-mode momenta  $P_j$  are small. But it is not too difficult to extend it to much larger values of these parameters. When  $P_j$  become comparable to  $\sqrt{n}$ , the vertex insertion in (3.1) must be treated as a part of the action, as it affects the saddle-point configurations. The saddle-point configuration(s) is still a constant field,  $\mathbf{X}(z, \bar{z}) = \mathbf{X}_0$ , but now  $\mathbf{X}_0$  is not an arbitrary point on the surface (1.11), but has to extremize the boundary action (3.4), which for constant fields takes the form

$$\mathcal{B}[\mathbf{X}_0] = -i \mathbf{P} \cdot \mathbf{X}_0. \quad (3.17)$$

Therefore, the saddle-points are the points where the tangent plane to the pillow surface is perpendicular to the vector  $\mathbf{P}$ . The dominating saddle point is easier to identify in the case of pure imaginary  $\mathbf{P}$ : it is the point of the real-space pillow surface farthest in the direction of  $-i \mathbf{P}$ . Contribution of this point can be determined as follows. The saddle-point action, together with the Gaussian integral over the constant mode can be simply taken from the asymptotic  $\alpha, \beta, \gamma \rightarrow -i\infty$  of the expression (3.9), since the asymptotic of the integral (3.10) is controlled by the very same saddle point. However, when  $(P_1, P_2, P_3) \sim \sqrt{n}$  the Gaussian integrals over the non-constant modes can not be ignored. For small deviations from the saddle point  $\mathbf{X}_0$ , let us write

$$\mathbf{X}(z, \bar{z}) - \mathbf{X}_0 = \mathbf{e}_j(\mathbf{X}_0) \xi^j(z, \bar{z}) + \mathbf{n}(\mathbf{X}_0) \delta X_{\perp}(z, \bar{z}), \quad (3.18)$$

where we assume that the vectors  $\mathbf{e}_j(\mathbf{X}_0)$  tangent to the pillow surface at  $\mathbf{X}_0$ , together with the normal vector  $\mathbf{n}(\mathbf{X}_0)$ , form orthonormal basis in  $\mathbb{R}^3$ . Furthermore, we choose  $\mathbf{e}_j(\mathbf{X}_0)$  in such a way that in the quadratic approximation

$$\left[ \delta X_{\perp} + K_1^{(0)} \frac{(\xi^1)^2}{2} + K_2^{(0)} \frac{(\xi^2)^2}{2} \right]_B = 0, \quad (3.19)$$

where  $K_j^{(0)}$  are principal curvatures of the pillow at  $\mathbf{X}_0$ . Then the Gaussian term in the full boundary action takes the form

$$\mathcal{A}_B + \mathcal{B} = \oint_{|z|=R} \frac{d\tau}{2\pi} \left[ \frac{m_1}{2R} (\xi^1)^2 + \frac{m_2}{2R} (\xi^1)^2 - i B_n^{(0)} \varepsilon_{ij} \xi^i \partial_\tau \xi^j \right], \quad (3.20)$$

where

$$m_j = -| -i\mathbf{P} | K_j^{(0)}, \quad (3.21)$$

and  $B_n^{(0)}$  the normal component of  $\mathbf{B}(\mathbf{X}_0)$ .

We see that, while to the leading approximation the normal component  $\delta X_\perp$  of the field  $\mathbf{X}$  still can be treated with the Dirichlet boundary condition, the tangential components  $\delta \mathbf{X}$  have free boundary conditions with the “boundary mass terms” in (3.20). Note that for  $m_j \sim 1$  (the condition which we assume) the energy scale associated with this “boundary mass” is  $\sim R^{-1}$ , so that the use of the renormalized parameters  $w$  defined as in (2.21) is still legitimate. The boundary amplitude of the free field with quadratic boundary interaction is well known (see [13, 14]). One finds that Eq.(3.13) would apply to the case of  $(P_1, P_2, P_3) \sim \sqrt{n}$  as well if one simply replaces  $B_{\text{class}} = B_{\text{class}}(\alpha, \beta, \gamma)$  in (3.13) by

$$\tilde{B}_{\text{class}} = B_{\text{class}} \left( \frac{\sqrt{n\nu}}{2} P_1, \frac{\sqrt{n(1-\nu)}}{2} P_2, \frac{\sqrt{n}}{2} P_3 \right) \Gamma\left(1 - \frac{i\Pi_1}{\sqrt{n}}\right) \Gamma\left(1 - \frac{i\Pi_2}{\sqrt{n}}\right), \quad (3.22)$$

where

$$\begin{aligned} \Pi_1 &= \frac{1 + w_1}{\nu - (1 - \nu) w_1} \sqrt{U(w_1)} \\ \Pi_2 &= \frac{1 + w_2}{(1 - \nu) w_2 - \nu} \sqrt{U(w_2)}, \end{aligned} \quad (3.23)$$

with

$$U(w) = \frac{\nu P_1^2 + w(1 - \nu) P_2^2}{1 + w} + \frac{w P_3^2}{(1 + w)^2}. \quad (3.24)$$

In Eq.(3.23) the branch of the square root should be chosen in such a way that  $\Im m \Pi_{1,2} > 0$  for pure imaginary  $P_{1,2}$  with  $\Im m P_{1,2} > 0$ . Of course in this case the arguments of  $B_{\text{class}}$  in (3.22) are large, and one can use the asymptotic forms of (3.14) and (3.15).

## 4 Ultraviolet limit of the pillow-brane model

As was mentioned in Introduction, at short length scales the  $w_1$  and  $w_2$  in (1.11) tend to 0 and to  $\infty$ , respectively. Correspondingly, the pillow surface grows wide in the  $X$  and  $Y$  directions, while its size in the  $Z$  direction approaches  $\pi \sqrt{n+2}$ . In this limit the pillow can be regarded as a juxtaposition of four “corners”, as is shown in Fig. 3. Any two adjacent corners are connected to each other via the “hairpin cylinder”. By this term we understand intrinsically flat surface obtained by tensoring  $\mathbb{R}$  and the “hairpin curve” defined in Ref. [8]. There are four hairpin cylinders in the UV limiting form of the pillow, which we label (1, 2), (2, 3), (3, 4), and (4, 1), as shown in Fig. 4.

When the pillow is wide, and if  $\Im m P_1$  and  $\Im m P_2$  are not too small, the functional integral in (3.3) is dominated by fields localized near one of the corners in Fig. 3. Which one of the four corners contributes depends on the signs of  $\Im m P_1$  and  $\Im m P_2$ . It is useful therefore to describe the boundary states associated with the “corner” and “hairpin cylinder” branes in some details.

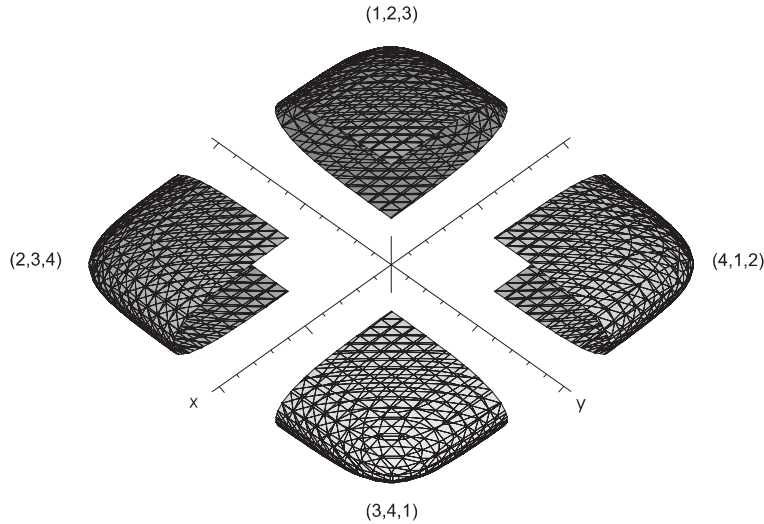


Figure 3: The pillow viewed as the composition of four "corners".

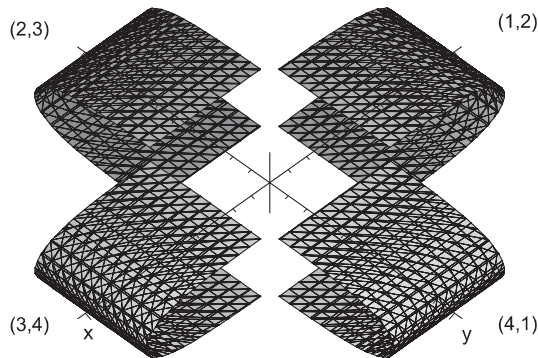


Figure 4: Four hairpin cylinders

#### 4.1 Hairpin cylinder

As the hairpin cylinder surface is a direct product of a line and the hairpin curve, all basic properties of the associated boundary state can be taken from Ref. [8]. Let us consider first the hairpin cylinder (1, 2). This surface is defined by the equation

$$\cos\left(\frac{Z_B}{\sqrt{n+2}}\right) = \tilde{a} \exp\left(-\frac{X_B}{\sqrt{nv}}\right), \quad (4.1)$$

where

$$\tilde{a} = \kappa^{\frac{1}{nv}}, \quad (4.2)$$

and  $\kappa = E_* R$ , while the field  $\mathbf{B}$  in this case is a constant vector pointing in the  $X$  direction,

$$\mathbf{B} = i(-\sqrt{1-\nu}, 0, 0). \quad (4.3)$$

The constraint (4.1) does not involve  $Y_B$ , i.e., the field  $Y$  obeys the free (von Neumann) boundary condition.

The RG flow just shifts the hairpin cylinder homogeneously in the  $X$  direction, and therefore this boundary condition is equivalent to a fixed point of the RG transformation. This fact is made explicit by redefining the RG transformation by supplementing it with the field redefinition  $(X, Y, Z) \rightarrow (X + \frac{\delta t}{\sqrt{n\nu}}, Y, Z)$ . This corresponds to introducing the linear dilaton  $\Phi(\mathbf{X}) = -\frac{X}{\sqrt{n\nu}}$ , or, which is much the same, adding the “improvement” term to the energy-momentum tensor,

$$\begin{aligned} T(z) &= -\partial_z \mathbf{X} \cdot \partial_z \mathbf{X} - \frac{1}{\sqrt{n\nu}} \partial_z^2 X, \\ \bar{T}(\bar{z}) &= -\partial_{\bar{z}} \mathbf{X} \cdot \partial_{\bar{z}} \mathbf{X} - \frac{1}{\sqrt{n\nu}} \partial_{\bar{z}}^2 X. \end{aligned} \quad (4.4)$$

With this, the boundary state  $|B\rangle_{(1,2)}$  associated with the hairpin cylinder brane enjoys conformal invariance in the usual form,

$$\left[ z^2 T(z) - \bar{z}^2 \bar{T}(\bar{z}) \right]_{|z|=R} |B\rangle_{(1,2)} = 0. \quad (4.5)$$

The hairpin cylinder brane has an extended conformal symmetry (the W-algebra). In fact, there are many ways to introduce the W-algebra in this theory, but only one is useful for our purposes here. We will call it  $\mathcal{W}^{(1,2)}$ -algebra, with the superscript  $(1,2)$  placed as the reminder that it belongs to the hairpin cylinder  $(1,2)$ . The algebra  $\mathcal{W}^{(1,2)}$  is generated by holomorphic currents  $W_s$  of spin  $s$  characterized by the condition that they commute with two “screening charges”,

$$\oint_z dw W_s(z) e^{\alpha_j \cdot \mathbf{X}_R(w)} = 0 \quad (4.6)$$

for  $j = 1, 2$ , where

$$\begin{aligned} \alpha_1 &= (-\sqrt{n\nu}, -\sqrt{n(1-\nu)}, i\sqrt{n+2}) \\ \alpha_2 &= (-\sqrt{n\nu}, \sqrt{n(1-\nu)}, -i\sqrt{n+2}). \end{aligned} \quad (4.7)$$

The integration in Eq.(4.6) is taken over a small contour around the point  $z$ . The subscript  $R$  stands for the holomorphic part of the local field  $\mathbf{X}(z, \bar{z}) = \mathbf{X}_R(z) + \mathbf{X}_L(\bar{z})$ . The full W-algebra  $\mathcal{W}^{(1,2)}$  can be generated by OPE of three basic currents, the spin-2 energy-momentum tensor  $W_2 \equiv T$  (given by (4.4)), and the spin-1 and spin-3 currents

$$\begin{aligned} W_1(z) &= i\sqrt{n+2} \partial_z Y + \sqrt{n(1-\nu)} \partial_z Z, \\ W_3(z) &= \frac{3n\nu+2}{3} (\partial_z \hat{Z})^3 + n\nu (\partial_z X)^2 \partial_z \hat{Z} - \\ &\quad \frac{n\nu\sqrt{n\nu}}{2} \partial_z^2 X \partial_z \hat{Z} + \frac{(n\nu+2)\sqrt{n\nu}}{2} \partial_z X \partial_z^2 \hat{Z} + \frac{n\nu+2}{12} \partial_z^3 \hat{Z}, \end{aligned} \quad (4.8)$$

where

$$\partial_z \hat{Z} = \sqrt{\frac{n+2}{n\nu+2}} \partial_z Z + i \sqrt{\frac{n(1-\nu)}{n\nu+2}} \partial_z Y. \quad (4.9)$$

the higher currents  $W_s$  can be found either by a direct computation of the OPE with the screening exponentials (4.7) (the condition (4.6) is equivalent to the statement that the singular part of the OPE of  $W_s(z) e^{\alpha_j \cdot \mathbf{X}_R(w)}$  is a total derivative  $\partial_w(\dots)$ ), or recursively, from the singular parts of the

OPE of the lower currents, starting with  $W_1$ ,  $W_2$  and  $W_3$ . Note that although the component  $Y$  of the field  $\mathbf{X}$  largely plays the role of a spectator in the dynamics of the hairpin cylinder (1, 2), this component is mixed in a nontrivial way in the currents  $W_s$ .

There is of course an antiholomorphic counterpart of the W-algebra  $\mathcal{W}^{(1,2)}$ , defined by the relations (4.6) with  $\bar{z}, \bar{w}$  instead of  $z, w$ ,  $\mathbf{X}_R(z)$  replaced by  $\mathbf{X}_L(\bar{z})$ , and  $\alpha_1, \alpha_2$  changed to

$$\begin{aligned}\bar{\alpha}_1 &= \left( -\sqrt{n\nu}, -\sqrt{n(1-\nu)}, -i\sqrt{n+2} \right), \\ \bar{\alpha}_2 &= \left( -\sqrt{n\nu}, \sqrt{n(1-\nu)}, i\sqrt{n+2} \right).\end{aligned}\tag{4.10}$$

The antiholomorphic currents  $\bar{W}_s(\bar{z})$  can be obtained from  $W_s(z)$  by replacing  $\partial_z X, \partial_z Y \rightarrow \partial_{\bar{z}} X, \partial_{\bar{z}} Y$ , and  $\partial_z Z \rightarrow -\partial_{\bar{z}} Z$ , for instance

$$\bar{W}_1(\bar{z}) = i\sqrt{n+2}\partial_{\bar{z}} Y - \sqrt{n(1-\nu)}\partial_{\bar{z}} Z.\tag{4.11}$$

The W-algebra symmetry of the boundary state associated with the hairpin cylinder (1, 2) is expressed as the set of local conditions

$$\left[ z^s W_s(z) - (-1)^s \bar{z}^s \bar{W}_s(\bar{z}) \right]_{|z|=R} |B\rangle_{(1,2)} = 0,\tag{4.12}$$

for all the W-currents in  $\mathcal{W}^{(1,2)}$ . At present, the status of this statement is as follows. We have verified directly that it is true in the classical limit  $n \rightarrow \infty$ , where the calculation amounts to checking that the differences  $z^s W_s(z) - (-1)^s \bar{z}^s \bar{W}_s(\bar{z})$ ,  $s = 1, 2, 3$  vanish at the boundary  $|z| = R$  in virtue of the classical equations corresponding to the action (1.1), (1.2),

$$\left( \partial_\tau \mathbf{X} - \frac{i}{B_n} \mathbf{n} \times \partial_\sigma \mathbf{X} \right) \Big|_{|z|=R} = 0,\tag{4.13}$$

together with the constraint (4.1). In Eq.(4.13)  $\partial_\tau X$  and  $\partial_\sigma \mathbf{X}$  stand for the tangential and internal normal derivative to the boundary circle  $|z| = R$ , respectively.

Other hairpin cylinders in Fig. 4 can be described in a similar way, with obvious modifications. The associated W-algebras are defined as follows. Introduce two additional vectors

$$\begin{aligned}\alpha_3 &= \left( \sqrt{n\nu}, -\sqrt{n(1-\nu)}, -i\sqrt{n+2} \right), \\ \alpha_4 &= \left( \sqrt{n\nu}, \sqrt{n(1-\nu)}, i\sqrt{n+2} \right).\end{aligned}\tag{4.14}$$

The W-algebras  $\mathcal{W}^{(2,3)}$ ,  $\mathcal{W}^{(3,4)}$ , and  $\mathcal{W}^{(4,1)}$  are generated by the W-currents which satisfy the conditions (4.6) with the pair of vectors  $\alpha_1, \alpha_2$  replaced by the corresponding pair  $\alpha_i, \alpha_j$ ,  $(i, j) = (2, 3), (3, 4), (4, 1)$ , respectively. Of course, all these W-algebras are isomorphic to each other, and differ only in the way they are embedded in the space of holomorphic fields of the bulk theory (1.1).

## 4.2 Corner-brane

More interesting conformal boundary conditions are represented by the ‘‘corner-branes’’, the corner surfaces in Fig. 3. There are four corners in Fig. 3, suggestively labeled by symbols (1, 2, 3), (2, 3, 4), (3, 4, 1), (4, 1, 2). Again we concentrate first on one of them, say the corner (1, 2, 3). This surface is described by the equation

$$\cos\left(\frac{Z_B}{\sqrt{n+2}}\right) = \tilde{a} \exp\left(-\frac{X_B}{\sqrt{n\nu}}\right) + \tilde{b} \exp\left(-\frac{Y_B}{\sqrt{n(1-\nu)}}\right),\tag{4.15}$$

where

$$\tilde{a} = \kappa \frac{1}{n\nu}, \quad \tilde{b} = \kappa \frac{1}{n(1-\nu)}, \quad (4.16)$$

and  $\kappa = E_* R$ .

Like the hairpin cylinder, the corner-brane boundary condition is equivalent to an RG fixed point. The RG flow can be ‘‘arrested’’ by redefining the RG transformation - supplementing with the shift  $(X, Y, Z) \rightarrow (X + \frac{\delta t}{\sqrt{n\nu}}, Y + \frac{\delta t}{\sqrt{n(1-\nu)}}, Z)$ . The corresponding linear dilaton has the form

$$\Phi(\mathbf{X}) = -\frac{X}{\sqrt{n\nu}} - \frac{Y}{\sqrt{n(1-\nu)}}. \quad (4.17)$$

In the presence of a dilaton field the one-loop RG flow equations (1.8),(1.9) are modified as follows [9]. The first of these equations receives an additional term,

$$\mathbf{n} \cdot \dot{\mathbf{X}}_B - \frac{K}{1 + B_n^2} - \mathbf{n} \cdot \nabla \Phi = 0, \quad (4.18)$$

whereas  $D_j$  in (1.9) are replaced by

$$D_j = (\mathbf{n} \cdot \dot{\mathbf{X}}_B) B_j + \frac{1}{1 + B_n^2} \frac{\partial B_n}{\partial \eta^j} - B_n \frac{\partial \Phi}{\partial \eta^j}. \quad (4.19)$$

The surface (4.17) solves the fixed point equations in the presence of the constant  $\mathbf{B}$  field,

$$\mathbf{B} = i \left( -\sqrt{1-\nu}, \sqrt{\nu}, 0 \right). \quad (4.20)$$

This can be checked for the one loop equations, but it likely holds to all loops.

#### 4.2.1 Corner-brane $W$ -algebra

The corner-brane boundary is conformally invariant. It is also very likely to have certain  $W$ -algebra symmetry. In this subsection we will identify the corner-brane  $W$ -algebra, using general arguments and consistency. Beyond the classical limit, we do not know how to derive the  $W$ -algebra directly from the boundary constraint (4.15). However, one can *define* the corner-brane boundary CFT by the  $W$ -algebra symmetry, and then check that its semiclassical limit agrees with Eqs.(4.13),(4.15). This is the strategy we adopt here.

Concentrating again on the corner brane (1, 2, 3) in Fig. 3, we observe that this surface incorporates two hairpin cylinders, (1, 2) and (2, 3) in Fig. 4, as the limiting cases. This suggests that the  $W$ -algebra associated with the corner brane (1, 2, 3) may include holomorphic currents  $W_s$  from  $\mathcal{W}^{(1,2)}$ , which also belong to  $\mathcal{W}^{(2,3)}$ . Thus, we define  $\mathcal{W}^{(1,2,3)} = \mathcal{W}^{(1,2)} \cap \mathcal{W}^{(2,3)}$ . In other words, the  $W$ -algebra  $\mathcal{W}^{(1,2,3)}$  consists of the currents  $W_s$  which satisfy the condition (4.6) with all three vertex operators  $\exp(\alpha_j \mathbf{X}_R)$ ,  $j = 1, 2, 3$ . This  $W$ -algebra is not new. It was introduced in Refs. [15, 16], and further studied in Ref. [17], where it was named  $\mathcal{WD}(2|1; \alpha)$ , with the parameter  $\alpha$  related to our  $\nu$  as  $\alpha = -\nu^{-1}$ . Its Virasoro central charge is

$$c = 3 + 6 \left( \frac{1}{n\nu} + \frac{1}{n(1-\nu)} - \frac{1}{n+2} \right). \quad (4.21)$$

Likewise, the  $W$ -algebras of the other corner branes in Fig. 3 are defined as the intersections of pairs of corresponding hairpin  $W$ -algebras, e.g.,  $\mathcal{W}^{(2,3,4)} = \mathcal{W}^{(2,3)} \cap \mathcal{W}^{(3,4)}$ , etc. Of course, as the



algebras, all these are isomorphic to  $\mathcal{W}^{(1,2,3)}$ , differing from it only in the way they are embedded in the space of the chiral fields of the bulk theory (1.1).

Let us describe here some properties of the algebra  $\mathcal{WD}(2|1; \alpha)$ , taking for definiteness its realization as  $\mathcal{W}^{(1,2,3)}$ . As usual, the number of independent holomorphic currents  $W_s$  of spin  $s$  can be read out of the character of the vacuum representation of this W-algebra [17],

$$\chi_{\text{vac}}(q) = 1 + q^2 + q^3 + 3q^4 + 3q^5 + 8q^6 + 9q^7 + 19q^8 + 25q^9 + \dots \quad (4.22)$$

Spin-1 currents are absent, but there is one spin-2 current

$$W_2 = -\partial_z \mathbf{X} \cdot \partial_z \mathbf{X} - \boldsymbol{\rho} \cdot \partial_z^2 \mathbf{X} \quad (4.23)$$

with

$$\boldsymbol{\rho} = \left( \frac{1}{\sqrt{nv}}, \frac{1}{\sqrt{n(1-\nu)}}, -\frac{i}{\sqrt{n+2}} \right), \quad (4.24)$$

which generates the Virasoro subalgebra with the above central charge. Furthermore, there is no truly independent spin-3 currents, since the only spin-3 field accounted in (4.22) is the derivative  $\partial_z W_2$ . At spin-4 there are three fields – two “descendant” currents,  $\partial_z^2 W_2$  and  $W_2^2$ , but also one new current  $W_4$ . By descendants here we understand the  $\partial_z$  derivatives and composite fields built from of the lower-spin currents.<sup>5</sup> Explicit form of  $W_4$  (first presented in [16]) is somewhat cumbersome, and we relegate it to Appendix. It will be important for our arguments below that it can be written as<sup>6</sup>

$$W_4 = W_4^{(\text{sym})} + \partial_z V_3, \quad (4.25)$$

where the non-derivative term  $W_4^{(\text{sym})}$  (but not  $V_3$ ) is symmetric with respect to all  $180^\circ$  rotations around the coordinate axes of the  $(X, Y, Z)$  space (equivalently, the simultaneous sign reversals of any pair of the fields  $(X, Y, X)$ ), and also respects the symmetries (1.15) and (1.16). Since these transformations interchange different corners in Fig. 3, this symmetry implies that the form of  $W_4^{(\text{sym})}$  is the same for all four realizations of the W-algebra, associated with the four corners.

It is likely (but not proven, or really verified beyond the spin 5) that similar structure persists to higher spins. Three-dimensional space of the spin-5 currents is spanned by the descendants, the  $\partial_z$  derivatives of the spin-4 currents. The eight-dimensional space of spin-6 currents involves seven descendants, and one new field, which again can be written in the form similar to (4.25),

$$W_6 = W_6^{(\text{sym})} + \partial_z V_5, \quad (4.26)$$

where  $W_6^{(\text{sym})}$  is symmetric under the rotations  $(X, Y, Z) \rightarrow (X, -Y, -Z), (-X, Y, -Z)$ . Going further up in the spins, we conjecture that there is exactly one independent current at each even spin, having the form

$$W_{2k} = W_{2k}^{(\text{sym})} + \partial_z V_{2k-1}, \quad (4.27)$$

in which the term  $W_{2k}^{(\text{sym})}$  is the same for all four realizations of the W-algebra associated with the four corners in Fig. 3.

---

<sup>5</sup>These are indeed descendants with respect to the W-algebra in the usual CFT sense: they are obtained from the identity operator by successive applications of the mode operators of the currents of the lower spins.

<sup>6</sup>The current (4.25) is not conformal primary, but can be made a primary by adding certain linear combination of  $W_2^2$  and  $\partial_z^2 W_2$ ; this form can be found in Ref. [17].

### 4.2.2 Boundary state of the corner-brane

As usual for conformal boundaries [11, 18, 19], the statement of the  $\mathcal{WD}(2|1; \alpha)$ -algebra symmetry of the boundary state associated with the corner-brane can be expressed as the set of equations

$$\left[ z^s W_s(z) - (-1)^s \bar{z}^s \bar{W}_s(\bar{z}) \right]_{|z|=R} |B\rangle_{(1,2,3)} = 0. \quad (4.28)$$

We have verified this equation only for  $s = 2$  and  $4$ , and only in the classical limit  $n \rightarrow \infty$ .<sup>7</sup>

It is sensible, however, to take (4.28) as a part of the definition of the corner-brane boundary. The the boundary state associated with, say, the corner-brane  $(1, 2, 3)$ , will then appear as the combination of the Ishibashi states  $|I_{\mathbf{P}}\rangle$  of the W-algebra  $\mathcal{W}^{(1,2,3)}$  (see e.g. [19] for the general notion),

$$|B\rangle_{(1,2,3)} = \int d\mathbf{P} B(\mathbf{P}) |I_{\mathbf{P}}\rangle_{(1,2,3)}, \quad (4.29)$$

where  $B(\mathbf{P})$  is the vacuum overlap of the corner-brane boundary state,  $B(\mathbf{P}) = \langle \mathbf{P} | B \rangle_{(1,2,3)}$ . Unlike the Ishibashi states, the amplitude  $B(\mathbf{P})$  is not determined by W-algebra alone. In principle, its form is restricted by the requirement of locality of the boundary interaction, but so far no direct way of solving for this condition is known. Similar problem was addressed in [8] for simpler case of the hairpin-brane, where exact form of the corresponding boundary overlap function was conjectured. Analogous expression for the corner-brane has the form

$$B(P_1, P_2, P_3) = \frac{g_D^3}{2\pi} \left( \frac{\kappa}{\alpha_1^2} \right)^{-i \frac{P_1}{\alpha_1}} \left( \frac{\kappa}{\alpha_2^2} \right)^{-i \frac{P_2}{\alpha_2}} \times \quad (4.30)$$

$$\frac{\sqrt{\alpha_1 \alpha_2} \Gamma(i \alpha_1 P_1) \Gamma(1 + i \frac{P_1}{\alpha_1}) \Gamma(i \alpha_2 P_2) \Gamma(1 + i \frac{P_2}{\alpha_2})}{\Gamma(\frac{1}{2} + i \frac{\alpha_1 P_1}{2} + i \frac{\alpha_2 P_2}{2} + i \frac{\alpha_3 P_3}{2}) \Gamma(\frac{1}{2} + i \frac{\alpha_1 P_1}{2} + i \frac{\alpha_2 P_2}{2} - i \frac{\alpha_3 P_3}{2})},$$

where

$$\alpha_1 = -\sqrt{n\nu}, \quad \alpha_2 = -\sqrt{n(1-\nu)}, \quad \alpha_3 = -i \sqrt{n+2}. \quad (4.31)$$

This expression passes several simple tests. Thus, it is straightforward to verify that in the semiclassical limit (4.30) agrees with the result of direct saddle-point calculation with the corner-brane boundary condition. Also, note the poles at  $P_1 = 0$  and  $P_2 = 0$  which signify the infinite extent of the brane in the  $X$  and  $Y$  directions. The residues at the poles coincide with the boundary amplitudes of the hairpin-branes of Ref. [8], in agreement with the fact that the corner-brane approaches the hairpin cylinders as in the limits  $X \rightarrow \infty$  or  $Y \rightarrow \infty$ . We conjecture that (4.30) is exact boundary amplitude of the corner-brane  $(1, 2, 3)$ .

The amplitude (4.30) applies to the corner-brane  $(1, 2, 3)$  in Fig. 3. The other corner branes are obtained from this one by simultaneous change of signs of two of the coordinates  $(X, Y, Z)$ . Therefore, the boundary amplitudes of the other branes in Fig. 3 are given by the same expression (4.30) with the signs of two of the components of  $\mathbf{P} = (P_1, P_2, P_3)$  reversed. For example  $\langle \mathbf{P} | B \rangle_{(2,3,4)} = B(-P_1, -P_2, P_3)$ .

---

<sup>7</sup>The leading term in the  $n \rightarrow \infty$  asymptotic of  $W_4$  in Eq.(A.1) is proportional to  $W_2^2$ ; for this term the equation (4.28) with  $s = 4$  is a simple consequence of the  $s = 2$  equation, and thus does not imply any additional symmetry beyond the conformal invariance. However, the combination  $\tilde{W}_4 = (W_4 + 9n^3\nu(1-\nu)W_2^2)/n^4$  has nontrivial  $n \rightarrow \infty$  limit, independent from  $W_2$ . It is for this current  $\tilde{W}_4$  that we have checked that  $z^4 \tilde{W}_4 - \bar{z}^4 \tilde{W}_4$  vanishes in virtue of the classical boundary conditions of the corner-brane.

## 5 Integrability of the pillow-brane model

In this section we will argue that the pillow-brane model is integrable. The following discussion is closely parallel to that presented in Ref. [8] in the context of the “paperclip model”, therefore we will be brief.

Let us first remind what we mean by the statement of integrability in this situation. In the bulk, we are dealing with the theory of free bosons which is trivially integrable. In particular, the bulk theory has infinite number of commuting integrals of motion. The relevant integrals of motion look simpler in terms of the coordinates  $(v, \bar{v}) = (\tau + i\sigma, \tau - i\sigma)$  related to  $(z, \bar{z})$  via the logarithmic conformal transformation

$$v = -iR \log(z/R), \quad \bar{v} = iR \log(\bar{z}/R), \quad (5.1)$$

which maps the disk  $|z| < R$  onto the semi-infinite cylinder  $\tau \equiv \tau + 2\pi R$ ,  $\sigma > 0$ , with the boundary placed at  $\sigma = 0$ . The exponential field insertion in (1.22) is equivalent to the condition that the shifted field  $\mathbf{X} - i\frac{\sigma}{R}\mathbf{P}$  (or (3.2)) is bounded on the cylinder. The space of holomorphic fields of the bulk theory is spanned by polynomials  $P(v) = P(\partial_v X^j, \partial_v^2 X^j, \dots)$  of the components of  $\partial_v \mathbf{X}$  and higher  $\partial_v$  derivatives of  $X^j$ . Integrating such polynomials over closed contour around the cylinder one obtains integrals of motion (IM)  $\mathbb{I}[P] = \oint \frac{dv}{2\pi} P(v)$  of the bulk theory. In the Hamiltonian picture with the coordinate  $\sigma$  along the cylinder taken as the “time”, the integrals  $\mathbb{I}[P]$  are operators acting in the space (1.21). Let  $P_{s+1}(v)$  be a set of polynomials such that the associated integrals

$$\mathbb{I}_s = \oint \frac{dv}{2\pi} P_{s+1}(v) \quad (5.2)$$

all commute,  $[\mathbb{I}_s, \mathbb{I}_{s'}] = 0$ . We say that a boundary condition at  $\sigma = 0$  is consistent with the set of IM  $\{\mathbb{I}_s\}$  if the corresponding boundary state  $|B\rangle$  satisfies the equations [20]

$$(\mathbb{I}_s - \bar{\mathbb{I}}_s) |B\rangle = 0, \quad (5.3)$$

where  $\bar{\mathbb{I}}_s = \oint \frac{d\bar{v}}{2\pi} \bar{P}_s(\bar{v})$  are the corresponding “left-moving” IM, obtained from  $\mathbb{I}_s$  by replacing  $v \rightarrow \bar{v}$ .<sup>8</sup> A boundary theory is integrable if it is consistent with a “maximal” set of commuting IM. By definition, any IM  $\mathbb{I}[P]$  which commutes with all members of the maximal set is a linear combination thereof. Generally, a free boson theory admits more than one maximal set. The maximal commuting set  $\{\mathbb{I}_s\}$  is the most important characteristic of an integrable boundary theory. In this section we identify what we believe is the commuting set associated with the pillow brane model.

### 5.1 Integrals of motion of the pillow-brane model

As usual, we assume that the subscript  $s$  indicates the Lorentz spin of the IM  $\mathbb{I}_s$ . First of all, the maximal commuting set  $\{\mathbb{I}_s\}$  always include the the spin-1 operator

$$\mathbb{I}_1 = - \oint \frac{dv}{2\pi} (\partial \mathbf{X})^2, \quad (5.4)$$

---

<sup>8</sup>Eq.(5.3) implies that the differences  $P_{s+1}(v) - \bar{P}_{s+1}(\bar{v})$ , when specified to the boundary  $v = \bar{v} = \tau$ , reduce to total derivatives  $\partial_\tau Q_s(\tau)$  in virtue of the boundary conditions. These equations in turn lead to nontrivial integrals of motion in the Hamiltonian picture where  $\tau$  plays the role of (Matsubara) time. Indeed, it is easy to see that the quantities  $\int_0^\infty d\sigma (P_{s+1}(\tau + i\sigma) - \bar{P}_{s+1}(\tau - i\sigma)) + Q_s(\tau)$  are independent of  $\tau$  [20].

the light-cone component of the energy-momentum. To figure out what the higher-spin IM associated with the pillow brane could possibly be, recall that in the short-scale limit the pillow surface tends to a juxtaposition of four corner branes. As was explained in Section 4, the individual corner branes are conformal boundary conditions which enjoy the W-algebra symmetry. Since the IM  $\mathbb{I}_s$  of the bulk CFT do not involve any scale, they have to be the elements of all four W-algebras  $\mathcal{W}^{(a,b,c)}$  corresponding to the four corners  $(a, b, c) = (1, 2, 3), (2, 3, 4), (3, 4, 1), (4, 1, 2)$  in Fig. 3. Although  $\mathcal{W}^{(a,b,c)}$  are isomorphic to each other as the algebras, they have different realizations in terms of the chiral fields of (1.1). The  $W$ -currents of  $\mathcal{W}^{(a,b,c)}$  are defined by the relations (4.6) with three exponentials,  $j = a, b, c$ . This suggests that the currents  $P_{s+1}(v)$  in the IM  $\{\mathbb{I}_s\}$  must obey some similar relations with all four exponentials  $j = 1, 2, 3, 4$ . It is highly unlikely that any local current can satisfy exactly (4.6) with  $j = 1, 2, 3, 4$ . However, the desired IM are integrals (5.2), therefore it is sufficient to demand

$$\oint_z dw P_{s+1}(z) e^{\alpha_j \cdot \mathbf{X}_R(w)} = \partial_z F_s, \quad (5.5)$$

for  $j = 1, 2, 3, 4$ , where  $F_s$  are local fields. The set of currents  $P_{s+1}$  defined by this condition is definitely not empty: it is straightforward to verify that  $P_2 = -(\partial_v \mathbf{X})^2$ , and  $P_4 = W_4^{(\text{sym})}$  given by Eq.(A.1) satisfy (5.5). This result was previously obtained in [21] in connection with different model. Moreover, the results of [21] suggest that there is infinite set of currents  $P_{s+1}$  with  $s = 1, 3, 5, \dots, 2k - 1, \dots$  which satisfy (5.5). These are the currents  $W_{2k}^{(\text{sym})}$ ,  $k = 1, 2, \dots$  conjectured in Section 4, Eq.(4.27). Unfortunately, at the moment we do not know how to prove existence of the higher spin (i.e. beyond  $P_2$  and  $P_4$ ) currents with this property. Nonetheless we will proceed under assumption that an infinite set of currents  $P_{2k}$ ,  $k = 1, 2, 3, \dots$  satisfying (5.5) exists, and moreover that the associates IM  $\mathbb{I}_{2k-1}$  form a maximal commuting set. Then, the boundary state satisfying (5.3) has the general form

$$|B\rangle = \int_{\mathbf{P}} \sum_m B_m(\mathbf{P}) |m, \mathbf{P}\rangle \otimes \overline{|m, \mathbf{P}\rangle}, \quad (5.6)$$

where  $|m, \mathbf{P}\rangle$  are the orthonormalized<sup>9</sup> simultaneous eigenvectors of the operators  $\mathbb{I}_s$  in the space  $\mathcal{F}_{\mathbf{P}}$ .

Note that the transformations (1.15) and (1.16) act by permutations on the four exponentials  $e^{\alpha_j \cdot \mathbf{X}_R}$ ,  $j = 1, 2, 3, 4$ . Therefore the currents  $P_{s+1}$  defined by (5.5), and the IM  $\mathbb{I}_s$ , are expected to be invariant with respect to these transformations (these symmetries are explicit in the expression (A.1) for  $P_4$ ). It is these symmetries that suggest that Eqs.(1.11), (1.12) provide perturbatively exact description of the pillow-brane – it is the simplest expression with correct  $n \rightarrow \infty$  limit which respects these symmetries.

## 5.2 Infrared limit of the pillow-brane model

To facilitate the discussion in this section, it is convenient to use formal interpretation of the boundary state  $|B\rangle$  in terms of the associated *boundary state operator* (see e.g. [18, 19]). Isomorphism between the Fock spaces  $\mathcal{F}_{\mathbf{P}}$  and  $\bar{\mathcal{F}}_{\mathbf{P}}$  provides one to one correspondence between the states in  $\mathcal{F}_{\mathbf{P}} \otimes \bar{\mathcal{F}}_{\mathbf{P}}$  and operators in  $\mathcal{F}_{\mathbf{P}}$ . Let  $\mathbb{B}$  be the operator corresponding to the boundary state  $|B\rangle$ . Then Eq.(5.3) is equivalent to the commutativity

$$[\mathbb{B}, \mathbb{I}_s] = 0, \quad (5.7)$$

---

<sup>9</sup>Here and below we assume the standard normalization  $\langle m, \mathbf{P} | m', \mathbf{P}' \rangle = \delta_{m,m'} \delta^{(3)}(\mathbf{P} - \mathbf{P}')$ .

and Eq.(5.6) can be written as

$$\mathbb{B} = \sum_m B_m(\mathbf{P}) |m, \mathbf{P}\rangle \langle m, \mathbf{P}|. \quad (5.8)$$

Thus, the coefficients  $B_m(\mathbf{P})$  are interpreted as the eigenvalues of the boundary state operator,

$$\mathbb{B} |m, \mathbf{P}\rangle = B_m(\mathbf{P}) |m, \mathbf{P}\rangle. \quad (5.9)$$

The eigenvalue  $B_0(\mathbf{P})$  corresponding to the Fock vacuum  $|\mathbf{P}\rangle \equiv |0, \mathbf{P}\rangle$  in  $\mathcal{F}_{\mathbf{P}}$  coincides with the overlap (1.23).

Arguments completely parallel to those given in Ref. [8] (see Section 6 therein) for the paperclip model suggest the following large- $R$  expansion of the boundary state operator of the pillow-brane,

$$\log \mathbb{B} \asymp \log(g_D^3) - \sum_{k=0}^{\infty} C_k E_*^{1-2k} \mathbb{I}_{2k-1} \quad (5.10)$$

where  $\log(g_D^3) = -\frac{3}{4} \log 2$  is the boundary entropy [22] of the infrared fixed point (the Dirichlet boundary condition<sup>10</sup>,  $\mathbf{X}_B = \mathbf{0}$ ), and the (asymptotic) series involves all local IM  $\{\mathbb{I}_{2k-1}\}$ , with the first one  $\mathbb{I}_{-1}$  being the identity operator by definition. The dimensionless coefficients  $C_k$  are yet to be determined. Even without knowing the coefficients  $C_k$ , this expansion has much predictive power. In particular, it yields the infrared asymptotic expansion of the partition function

$$\log Z(\mathbf{P} | \kappa) \asymp \log(g_D^3) - \sum_{k=0}^{\infty} C_k \kappa^{1-2k} I_{2k-1}(\mathbf{P}), \quad (5.11)$$

where

$$I_{2k-1}(\mathbf{P}) = R^{2k-1} \langle \mathbf{P} | \mathbb{I}_{2k-1} | \mathbf{P} \rangle \quad (5.12)$$

are the dimensionless vacuum expectation values of the local IM. The expectation values incorporate all dependence on the components of the zero mode momentum  $\mathbf{P}$ . They are polynomials of the degree  $2k$  of the components  $(P_1, P_2, P_3)$ , which can be obtained by direct computations once explicit expressions for the currents  $P_{2k}$  are known. Thus, from  $P_2 = -(\partial_z \mathbf{X})^2$  and  $P_4 = W_4^{(\text{sym})}$  as given by Eq.(A.1) in Appendix, one finds

$$\begin{aligned} I_1(\mathbf{P}) &= \frac{P_1^2}{4} + \frac{P_2^2}{4} + \frac{P_3^2}{4} - \frac{1}{8}, \\ I_3(\mathbf{P}) &= \sum_{j=1}^3 E_j \left( \frac{P_j^4}{16} - \frac{P_j^2}{16} + \frac{1}{192} \right) + \sum_{m \neq j} E_{mj} \left( \frac{P_m^2}{4} - \frac{1}{24} \right) \left( \frac{P_j^2}{4} - \frac{1}{24} \right) + \\ &\quad \frac{1}{240} \sum_{j=1}^3 H_j, \end{aligned} \quad (5.13)$$

where the numerical coefficients  $E_j$ ,  $E_{mj}$  and  $H_j$  are given by (A.3).

---

<sup>10</sup> The expansion in terms of the local IM appears in integrable boundary theories which flow down to the “basic” boundary fixed point, the one which admits no primary boundary fields but the identity operator. In those theories the expansion in  $\mathbb{I}_s$  corresponds to expansion of the infrared effective action in terms of descendants of the identity. Clearly, the Dirichlet boundary is of that kind.

## 6 Proposal for the overlap amplitude $\langle \mathbf{P} | B \rangle$

In Ref. [8] exact expression for the boundary amplitude of the paperclip model was proposed in terms of solutions of certain linear ordinary differential equation. Here we present similar proposal for the pillow brane model, and test it against various known properties of the model. Similar constructions are known in a number of integrable boundary models, where the boundary states can be related to Baxter's operators [23] (for review see [24] and references therein). The relation of eigenvalues of Baxter's operators in CFT to ordinary differential equation was originally proposed in [25].

### 6.1 Differential equation

Consider the ordinary second order differential equation

$$\left[ -\frac{d^2}{dx^2} + V(x) \right] \Psi(x) = 0, \quad (6.1)$$

with

$$V(x) = \kappa^2 e^{-n\nu x} (1 + e^x)^n - \frac{\alpha^2 + \beta^2 e^x}{1 + e^x} - \left(\gamma^2 - \frac{1}{4}\right) \frac{e^x}{(1 + e^x)^2}. \quad (6.2)$$

The parameters  $\alpha$ ,  $\beta$  and  $\gamma$  here will be related to the components of the momentum  $\mathbf{P} = (P_1, P_2, P_3)$  in (1.22),

$$\alpha = \frac{1}{2} \sqrt{n\nu} P_1, \quad \beta = \frac{1}{2} \sqrt{n(1-\nu)} P_2, \quad \gamma = \frac{1}{2} \sqrt{n+2} P_3, \quad (6.3)$$

and  $\kappa$  is assumed to be the same as in (1.14). Below we always assume that  $\kappa$  is real and positive. In the semiclassical case  $n \gg 1$  the parameters  $\alpha$ ,  $\beta$ ,  $\gamma$  here are the same as in (3.5).

Let  $\Psi_-(x)$  be the solution of (6.1) which decays when  $x$  goes to  $-\infty$  along the real axis, and  $\Psi_+(x)$  be another solution of (6.1), the one which decays at large positive  $x$ . We fix normalization of these two solutions as follows,

$$\begin{aligned} \Psi_- &\rightarrow \kappa^{-\frac{1}{2}} e^{\Phi(\nu;x)} && \text{as } x \rightarrow -\infty, \\ \Psi_+ &\rightarrow \kappa^{-\frac{1}{2}} e^{\Phi(1-\nu;-x)} && \text{as } x \rightarrow +\infty, \end{aligned} \quad (6.4)$$

where

$$\Phi(\nu | x) = \frac{n\nu x}{4} - \frac{2\kappa}{n\nu} e^{-\frac{n\nu x}{2}} {}_2F_1\left(-\frac{n\nu}{2}, -\frac{n}{2}, 1 - \frac{n\nu}{2}; -e^x\right). \quad (6.5)$$

Let

$$W[\Psi_+, \Psi_-] \equiv \Psi_+ \frac{d}{dx} \Psi_- - \Psi_- \frac{d}{dx} \Psi_+ \quad (6.6)$$

be the Wronskian of these two solutions. Then, our proposal for the function (1.23) is

$$Z(\mathbf{P} | \kappa) = \frac{g_D^3}{2} W[\Psi_+, \Psi_-]. \quad (6.7)$$

In this section we present arguments supporting our proposal (6.7). This requires understanding some properties of the solution of the differential equation (6.1), (6.2).

## 6.2 Small $\kappa$

In the analysis below, it will be convenient to split the potential (6.2) into two parts,

$$V(x) = V_-(x) + V_+(x), \quad (6.8)$$

where

$$V_-(x) = -\frac{\alpha^2 + \beta^2 e^x}{1 + e^x} - \left(\gamma^2 - \frac{1}{4}\right) \frac{e^x}{(1 + e^x)^2}, \quad (6.9)$$

and

$$V_+(x) = \kappa^2 e^{-n\nu x} (1 + e^x)^n. \quad (6.10)$$

At large negative  $x$  the term  $V_-(x)$  approaches the constant  $-\alpha^2$ , while  $V_+(x)$  can be approximated as  $\kappa^2 e^{-n\nu x}$ . At small  $\kappa^2$ , the accuracy of the last approximation is understood after making the change of the variable  $x = x_0 - \frac{2}{n\nu} y$ , where  $x_0 = \frac{2}{n\nu} \log\left(\frac{2\kappa}{n\nu}\right)$ ; Eq. (6.1) then takes the form

$$\left[ -\frac{d^2}{dy^2} - \left(\frac{2\alpha}{n\nu}\right)^2 + e^{2y} + \delta V(y) \right] \Psi = 0, \quad (6.11)$$

where  $\delta V \sim \kappa \frac{2}{n\nu}$  as  $\kappa \rightarrow 0$ . Therefore for  $1 \ll -x$  we have

$$\Psi_-(x) = \frac{2}{\sqrt{\pi n\nu}} K_{\frac{2i\alpha}{n\nu}}\left(\frac{2\kappa}{n\nu} e^{-\frac{n\nu x}{2}}\right) + O\left(\kappa \frac{2}{n\nu}\right). \quad (6.12)$$

where  $K_\mu(z)$  is the Macdonald function. The normalization in Eq.(6.12) is chosen to agree with the asymptotic form (6.4). In the domain

$$1 \ll -x \ll \frac{1}{n\nu} \log\left(\frac{1}{\kappa^2}\right), \quad (6.13)$$

the solution  $\Psi_-$  (6.12) becomes a combination of two plane waves,

$$\Psi_-(x) = D_\nu(-\alpha) e^{+i\alpha x} + D_\nu(\alpha) e^{-i\alpha x}, \quad (6.14)$$

with

$$D_\nu(\alpha) = \frac{1}{\sqrt{\pi n\nu}} \left(\frac{\kappa}{n\nu}\right)^{\frac{2i\alpha}{n\nu}} \Gamma\left(-\frac{2i\alpha}{n\nu}\right) \left[1 + O\left(\kappa \frac{2}{n\nu}\right)\right]. \quad (6.15)$$

On the other hand, when  $\kappa$  goes to zero, and

$$-\frac{1}{n\nu} \log\left(\frac{1}{\kappa^2}\right) \ll x \ll \frac{1}{n(1-\nu)} \log\left(\frac{1}{\kappa^2}\right), \quad (6.16)$$

the term  $V_+$  in (6.8) is negligible. In this domain Eq.(6.1) reduces to the Riemann differential equation, and its solution  $\Psi_-$  specified by the asymptotic behavior (6.14) has the form

$$\Psi_-(x) = D_\nu(-\alpha) Q_{-\alpha, \beta, \gamma}(e^x) + D_\nu(\alpha) Q_{\alpha, \beta, \gamma}(e^x), \quad (6.17)$$

where  $Q_{\alpha, \beta, \gamma}(w)$  is the hypergeometric function (3.12). The solution  $\Psi_+$  can be obtained from  $\Psi_-$  by substitution  $\alpha \leftrightarrow \beta$ ,  $\nu \rightarrow 1 - \nu$  and  $x \rightarrow -x$ , i.e.,

$$\Psi_+(x) = D_{1-\nu}(-\beta) Q_{-\beta, \alpha, \gamma}(e^{-x}) + D_{1-\nu}(\beta) Q_{\beta, \alpha, \gamma}(e^{-x}). \quad (6.18)$$

Using

$$W[Q_{\beta,\alpha,\gamma}(e^{-x}), Q_{\alpha,\beta,\gamma}(e^x)] = \frac{\Gamma(1-2i\alpha)\Gamma(1-2i\beta)}{\Gamma(\frac{1}{2}-i\alpha-i\beta-\gamma)\Gamma(\frac{1}{2}-i\alpha-i\beta+\gamma)}. \quad (6.19)$$

we find the limiting  $\kappa \rightarrow 0$  form of (6.7),

$$\frac{g_D^3}{2} W[\Psi_+, \Psi_-] \rightarrow \sum_{\varepsilon, \varepsilon' = \pm 1} B(\varepsilon P_1, \varepsilon' P_2, \varepsilon \varepsilon' P_3), \quad (6.20)$$

where  $B(P_1, P_2, P_3)$  is exactly the boundary-state amplitude (4.30) of the corner-brane. This is expected form of the UV limit  $\kappa \rightarrow 0$  of the boundary amplitude of the pillow-brane model. Indeed, as was discussed in Section 4, in this limit the pillow surface becomes infinitely wide in the  $X$  and  $Y$  directions, and its shape near the round ends is well described by the corner-branes in Fig. 3. If the components  $P_1, P_2$  of the momentum have nonzero imaginary part, the exponential insertion in the functional integral (3.1) pulls the field towards one of the corners. This is why in the  $\kappa \rightarrow 0$  limit  $Z(\mathbf{P}|\kappa)$  must reduce to the corner brane amplitude. Which of the corners dominate depends on the signs of  $\Im m P_1$  and  $\Im m P_2$ , and the effect is expected to become more prominent at large  $n$ , where the classical configuration dominates. This  $\kappa \rightarrow 0$  limiting behavior is in full agreement with (6.20), where the factor  $\kappa^{\frac{i\varepsilon P_1}{\sqrt{n\nu}} + \frac{i\varepsilon' P_2}{\sqrt{n(1-\nu)}}$  in  $B(\varepsilon P_1, \varepsilon' P_2, \varepsilon \varepsilon' P_3)$  makes one of the terms in the sum dominate at nonzero  $\Im m P_1, \Im m P_2$ .

### 6.3 Semiclassical domain $1 \ll n, \kappa \ll 1$

It is possible to show that corrections to the  $\kappa \rightarrow 0$  limiting form (6.20) are expanded in powers of  $\kappa^{\frac{2}{n\nu}}$  and  $\kappa^{\frac{2}{n(1-\nu)}}$ . When  $\kappa$  is small but  $n$  is large, so that  $\kappa^{\frac{2}{n}} \sim 1$ , all terms in this expansion are to be collected. Let us assume that the roots  $w_1$  and  $w_2$  of the equation (1.12) are not too close to each other. This regime corresponds to the semiclassical domain of the paperclip model considered in Section 3.

First, let us consider the case when  $\alpha, \beta$  and  $\gamma$  in (6.2) are of the order of 1, and the semiclassical pillow-brane amplitude is given by Eq.(3.9). Under these conditions the term  $V_+(x)$  in the potential has the effect of rigid walls at some points  $x_1, x_2$  ( $x_1 < x_2$ ). That is, for  $x - x_1 \gg \frac{1}{n}$  and  $x_2 - x \gg \frac{1}{n}$ , the potential  $V_+(x)$  is negligible, but outside the segment  $(x_1, x_2)$  it grows fast, so that the solution  $\Psi_-(x)$  ( $\Psi_+(x)$ ) essentially vanishes at  $x < x_1$  ( $x > x_2$ ). It is possible to show that when  $1 \gg x - x_1 \gg 1/n$ , the solution  $\Psi_-(x)$  is well approximated by a linear function,

$$\Psi_-(x) \approx \chi_1 (x - x_1). \quad (6.21)$$

Similarly, when  $x$  is below but close to  $x_2$ , the solution  $\Psi_+(x)$  behaves as

$$\Psi_+(x) \approx \chi_2 (x_2 - x). \quad (6.22)$$

The positions  $x_1, x_2$  of the walls and the slopes  $\chi_{1,2}$  depend on  $\kappa$ ,

$$\chi_{1,2} = \sqrt{\frac{n}{\pi} \frac{|\nu - (1-\nu)w_{1,2}|}{(1+w_{1,2})}} \left(1 + O\left(\frac{1}{n}\right)\right), \quad (6.23)$$



and

$$x_{1,2} = \log(w_{1,2}) + O\left(\frac{1}{n}\right), \quad (6.24)$$

where  $w_{1,2}$  are two roots of the equation identical to the pillow-brane RG flow equation (1.12). We will derive these equations later in this section. Within the segment  $(x_1, x_2)$  the term  $V_+(x)$  can be neglected, and (6.1) reduces to hypergeometric equation. Its solutions  $\Psi_{\pm}(x)$  in this segment are uniquely determined by the corresponding ‘‘initial conditions’’ (6.21) and (6.22). Thus, for instance

$$\Psi_-(x) = \frac{\chi_1}{2i\alpha} \left( Q_{\alpha,\beta,\gamma}(w_1) Q_{-\alpha,\beta,\gamma}(e^x) - Q_{-\alpha,\beta,\gamma}(w_1) Q_{\alpha,\beta,\gamma}(e^x) \right), \quad x_1 < x < x_2. \quad (6.25)$$

To compute the Wronskian in (6.7), take  $x$  close to the right wall  $x_1$ , where both (6.21) and (6.25) are valid. Then

$$W[\Psi_+, \Psi_-] \approx \chi_2 \Psi_-(x_2). \quad (6.26)$$

With (6.25) and (6.23) this yields exactly Eq.(3.9). (Of course, one can make similar analysis in the vicinity of the left wall  $x_2$ , which leads to the same result.)

Next, consider the case  $P_1, P_2, P_3 \sim 1$ . The term  $V_+(x)$  still dominates outside the segment  $(x_1, x_2)$ , but can be neglected inside it, provided  $x - x_1 \gg \frac{1}{n}$  and  $x_2 - x \gg \frac{1}{n}$ . Take  $x$  in the vicinity of the left wall, i.e., in the domain  $|x - x_1| \ll 1$ . Here the term  $V_-(x)$  can be replaced by its value at  $x_1$ ,

$$V_-(x) \approx V_-(x_1) = -\frac{\pi^2}{4n} \chi_1^4 \Pi_1^2, \quad (6.27)$$

where  $\chi_1$  is given by (6.23) and  $\Pi_1$  is exactly the expression (3.23). On the other hand, in this domain the term  $V_+(x)$  behaves as the exponential

$$V_+(x) \approx \pi^2 \chi_1^4 e^{-2y}, \quad y = \frac{\pi \chi_1^2}{2} (x - x_1). \quad (6.28)$$

Therefore, at  $x$  close to  $x_1$  we have

$$\Psi_-(x) \approx \frac{2}{\pi \chi_1} K_{\frac{i\Pi_1}{\sqrt{n}}} (2e^{-y}), \quad (6.29)$$

where the normalization factor is fixed by matching the asymptotic form (6.4). For small  $\Pi_1/\sqrt{n}$  and  $y \gg 1$  (6.29) reduces to a linear function – this is how Eq.(6.21) was obtained. The solution (6.29) should be matched to (6.17) in the domain  $\frac{1}{n} \ll x - x_1 \ll 1$ , where both approximations are valid, and then continued to the right wall. Likewise, in the vicinity of the right wall, where  $|x - x_2| \ll 1$ , the solution  $\Psi_+$  is approximated as

$$\Psi_+(x) \approx \frac{2}{\pi \chi_2} K_{\frac{i\Pi_2}{\sqrt{n}}} (2e^{\tilde{y}}), \quad \tilde{y} = \frac{\pi \chi_2^2}{2} (x - x_2), \quad (6.30)$$

where  $\Pi_2$  and  $\chi_2$  are given by (3.23) and (6.23) respectively. Then the Wronskian in (6.7) can be evaluated in the domain  $\frac{1}{n} \ll x_2 - x \ll 1$ ; the result is exactly (3.13) with  $B_{\text{class}}$  replaced by  $\tilde{B}_{\text{class}}$ , Eq.(3.22).

## 6.4 Large $\kappa$

At large  $\kappa$  WKB approximation for the solutions of (6.1) is valid. Standard calculations within the WKB expansion [26] yield for the Wronskian (6.6)

$$\begin{aligned} \log W &= \log(2) + \frac{\Gamma(-\frac{\alpha_1^2}{2})\Gamma(-\frac{\alpha_2^2}{2})}{\Gamma(1 + \frac{\alpha_3^2}{2})} \kappa + \\ &\int_{-\infty}^{\infty} dx \left\{ \kappa (\mathcal{P}(x) - \mathcal{P}_0(x)) + \frac{1}{8\kappa} \frac{(\mathcal{P}'(x))^2}{\mathcal{P}^3(x)} + \dots \right\}, \end{aligned} \quad (6.31)$$

where  $\mathcal{P}(x) = \kappa^{-1} \sqrt{V(x)}$  and we use the notations (4.31). The term with  $\mathcal{P}_0(x) = e^{-\frac{n\nu x}{2}} (1 + e^x)^{\frac{n}{2}}$  is subtracted in order to take into account the asymptotic conditions (6.4). With the explicit form (6.8) of the potential, Eq.(6.2) yields asymptotic expansion of the partition function (5.11) which has the form (5.11) with

$$C_k = \frac{\Gamma(k - \frac{1}{2})}{\sqrt{\pi} (2k - 1) 2^{3(k-1)}} \frac{\Gamma(1 + \alpha_1^2(k - \frac{1}{2})) \Gamma(1 + \alpha_2^2(k - \frac{1}{2}))}{\Gamma(-\alpha_3^2(k - \frac{1}{2}))}, \quad (6.32)$$

and  $I_{2k-1}(\mathbf{P})$  being certain polynomials of the variables  $P_1^2$ ,  $P_2^2$  and  $P_3^2$  (related to  $\alpha, \beta, \gamma$  as in (6.3)) of the degree  $2k$ . The highest-order terms in these polynomials are determined by the first term in the integrand in (6.31),

$$\begin{aligned} I_{2k-1}(\mathbf{P}) &= \frac{(-2)^{k-1}}{(2k-1)^2 (\alpha_1 \alpha_2 \alpha_3)^2} \sum_{i+j+l=k} (\alpha_1 P_1)^{2i} (\alpha_2 P_2)^{2j} (\alpha_3 P_3)^{2l} \times \\ &\frac{(\alpha_1^2 (k - \frac{1}{2}))_{k-i} (\alpha_2^2 (k - \frac{1}{2}))_{k-j} (\alpha_3^2 (k - \frac{1}{2}))_{k-l}}{i! j! l!} + \dots \quad (k \geq 0), \end{aligned} \quad (6.33)$$

where we use the notation

$$(x)_j = \frac{\Gamma(x+j)}{\Gamma(x)}. \quad (6.34)$$

This expression is in perfect agreement with the highest-order terms of the polynomials (5.13) obtained directly from the lowest spin IM. Moreover, it is straightforward to generate the full polynomials  $I_{2k-1}(\mathbf{P})$  evaluating the integral (6.31) order by order in  $\kappa^{-2}$ . This calculation reproduces the eigenvalues (5.13) in all details. This seems to be highly nontrivial test of our proposal. It would be interesting to find higher spin representatives of the commuting set  $\{\mathbb{I}_{2k-1}\}$ , and compare their vacuum eigenvalues with the higher polynomials  $I_{2k-1}(\mathbf{P})$  in the WKB expansion (6.6). Note that our proposal predicts exact values of the coefficients  $C_k$  in (5.11).

## 6.5 $U(1)$ -invariant limit

As was mentioned in Introduction, in the limit  $n \rightarrow \infty$ ,  $\nu \rightarrow 0$  with the parameters  $\lambda = n\nu$  and  $\bar{\kappa}^2 = \kappa^2 \nu^{-\lambda} \lambda^{-2}$ , the pillow (1.11) becomes a surface of revolution (1.17). It is interesting to look at the differential equation (6.1) in this limit.

If  $n$  goes to  $\infty$  while  $\kappa$  remains fixed, the term  $V_+(x)$  in the potential (6.8) becomes infinite at any finite  $x$ . Interesting limit is obtained by making first the shift of  $x$ ,

$$x = y + \log(\nu), \quad (6.35)$$

so that  $V_+(x) = \kappa^2 \nu^{-\lambda} e^{-\lambda y} (1 + \nu e^y)^n$ . Then the limit  $n \rightarrow \infty$  brings the equation (6.1) to the form

$$\left[ -\frac{d^2}{dy^2} - \frac{\lambda}{4} (P_{\parallel}^2 + P_{\perp}^2 e^y) + \bar{\kappa}^2 \exp(\lambda(e^y - y)) \right] \Psi(y) = 0, \quad (6.36)$$

where  $P_{\parallel} = P_1$ ,  $P_{\perp}^2 = P_2^2 + P_3^2$ . Thus, our proposal (6.7) applies directly to the  $U(1)$ -invariant brane (1.17), with  $W[\Psi_+, \Psi_-]$  defined as the Wronskian of two solutions of the differential equation (6.36) specified by the asymptotic conditions

$$\Psi_-(y) \rightarrow \bar{\kappa}^{-\frac{1}{2}} \exp\left(\frac{\lambda}{4} y - 2\bar{\kappa} e^{-\frac{\lambda}{2} y} G\left(\frac{\lambda}{2} e^y\right)\right) \quad \text{as } y \rightarrow -\infty, \quad (6.37)$$

and

$$\Psi_+(y) \rightarrow \bar{\kappa}^{-\frac{1}{2}} \exp\left(\frac{\lambda}{4} (y - e^y) + 2\bar{\kappa} e^{-\frac{\lambda}{2} y} G\left(\frac{\lambda}{2} e^y\right)\right) \quad \text{as } y \rightarrow +\infty. \quad (6.38)$$

Here  $G(y)$  is the confluent hypergeometric function,

$$G(z) = {}_1F_1\left(-\frac{\lambda}{2}, 1 - \frac{\lambda}{2}; z\right). \quad (6.39)$$

Finally, if one sets

$$y = \frac{v}{\sqrt{\lambda}}, \quad (6.40)$$

and takes the limit  $\lambda \rightarrow \infty$  with fixed  $z$  and  $\tilde{\kappa}^2 = \bar{\kappa}^2 \lambda e^{\lambda}$ , the differential equation (6.36) reduces to

$$\left[ -\frac{d^2}{dv^2} - \frac{\mathbf{P}^2}{4} + \tilde{\kappa}^2 e^{v^2/2} \right] \Psi(z) = 0. \quad (6.41)$$

This is exactly the differential equation proposed in Ref. [7] in relation to the spherical-brane model.

## Acknowledgments

Many key points in this work have emerged as the development of ideas of Alexei Zamolodchikov and we were privileged to discuss them with him.

We are grateful to Vladimir Bazhanov and Vladimir Fateev for their interest to this work, and to Dmitri Belov for help with graphic software. SL also acknowledges discussions with Dmitri Belov, Greg Moore, Nikita Nekrasov and Alexei Tsvetik.

This research is supported in part by DOE grant #DE-FG02-96 ER 40959. SL also acknowledges support from Institute for Strongly Correlated and Complex Systems at BNL where the part of this work was done in March 2003.

## A The current $W_4$ in Eq.(4.25)

Here we present explicit expression for the current  $W_4$  in Section 4. The two terms in (4.25) involve

$$\begin{aligned}
W_4^{(\text{sym})} &= \sum_{j=1}^3 E_j (\partial_z X^j)^4 + \sum_{m \neq j} E_{mj} (\partial_z X^m)^2 (\partial_z X^j)^2 \\
&+ \sum_{j \neq k \neq m} K_j \partial_z^2 X^j \partial_z X^k \partial_z X^m + \sum_{j=1}^3 H_j (\partial_z^2 X^j)^2
\end{aligned} \tag{A.1}$$

and

$$\begin{aligned}
V_3 &= \sum_{j=1}^3 K'_j (\partial_z X^j)^3 + \sum_{m \neq j} K'_{mj} \partial_z X^m (\partial_z X^j)^2 \\
&+ \sum_{j=1}^3 H'_j \partial_z^2 X^j \partial_z X^j + \sum_{m \neq j} H'_{mj} \partial_z^2 X^m \partial_z X^j + \sum_{j=1}^3 F'_j \partial_z^3 X^j.
\end{aligned} \tag{A.2}$$

In these equations ( $X^1, X^2, X^3$ ) stand for ( $X, Y, Z$ ), and the coefficients are expressed through three numbers (4.31) as follows,

$$\begin{aligned}
E_j &= -\alpha_j^2 (3\alpha_m^2 + 2)(3\alpha_k^2 + 2), \\
E_{mj} &= -3\alpha_m^2 \alpha_j^2 (3\alpha_k^2 + 2), \\
K_j &= -2\alpha_1 \alpha_2 \alpha_3 (3\alpha_j^2 + 2), \\
H_j &= 8 - \alpha_j^4 - 9(\alpha_1^2 \alpha_2^2 + \alpha_2^2 \alpha_3^2 + \alpha_3^2 \alpha_1^2) - 15\alpha_1^2 \alpha_2^2 \alpha_3^2,
\end{aligned} \tag{A.3}$$

and

$$\begin{aligned}
K'_j &= \frac{2}{3} \alpha_j (3\alpha_m^2 + 2)(3\alpha_k^2 + 2), \\
K'_{mj} &= 2\alpha_m \alpha_j^2 (3\alpha_k^2 + 2), \\
H'_j &= \alpha_j^2 (2\alpha_m^2 + 2\alpha_k^2 + 5\alpha_m^2 \alpha_k^2) \\
H'_{mj} &= 2\alpha_m \alpha_j (\alpha_m^2 - \alpha_k^2) \\
F'_j &= -\frac{1}{3} \alpha_j^3,
\end{aligned} \tag{A.4}$$

In these equations ( $j, k, m$ ) represent any permutation of the numbers (1, 2, 3).

## References

- [1] J. Polchinski, ‘‘Tasi lectures on D-branes,’’ Preprint NSF-ITP-96-145, 63 pp. [arXiv:hep-th/9611050].
- [2] C. G. Callan, Jr. and L. Thorlacius, Nucl. Phys. B **329**, 117 (1990).
- [3] I. Bakas, ‘‘Renormalization group equations and geometric flows’’ [arXiv:hep-th/0702034].
- [4] R. Hamilton, J. Differential Geom. **17**(2), 255 (1982).

- [5] G. Perelman, “The entropy formula for the Ricci flow and its geometric applications” [arXiv:math.DG/0211159]; “Ricci flow with surgery on three-manifolds” [arXiv:math.DG/0303109].
- [6] D. Friedan, Phys. Rev. Lett. **45**, 1057 (1980); Annals Phys. **163**, 318 (1985).
- [7] S. L. Lukyanov and A. B. Zamolodchikov, J. Stat. Mech. **0405**, P05003 (2004) [arXiv:hep-th/0306188].
- [8] S. L. Lukyanov, E. S. Vitchev and A. B. Zamolodchikov, Nucl. Phys. B **683**, 423 (2004) [arXiv:hep-th/0312168].
- [9] R. G. Leigh, Mod. Phys. Lett. A **4**, 2767 (1989).
- [10] C. G. Callan, Jr., C. Lovelace, C. R. Nappi and S. A. Yost, Nucl. Phys. B **293**, 83 (1987).
- [11] C. G. Callan, Jr., C. Lovelace, C. R. Nappi and S. A. Yost, Nucl. Phys. B **308**, 221 (1988).
- [12] E. S. Fradkin and A. A. Tseytlin, Phys. Lett. B **163**, 123 (1985).
- [13] E. Witten, Phys. Rev. D **47**, 3405 (1993) [arXiv:hep-th/9210065].
- [14] O. Andreev, Nucl. Phys. B **598**, 151 (2001) [arXiv:hep-th/0010218].
- [15] V.A. Fateev, unpublished.
- [16] V. A. Fateev, Nucl. Phys. B **473**, 509 (1996).
- [17] B. L. Feigin and A. M. Semikhatov, Nucl. Phys. B **610**, 489 (2001) [arXiv:hep-th/0102078].
- [18] N. Ishibashi, Mod. Phys. Lett. A **4**, 251 (1989).
- [19] J. L. Cardy, Nucl. Phys. B **324**, 581 (1989).
- [20] S. Ghoshal and A. B. Zamolodchikov, Int. J. Mod. Phys. A **9**, 3841 (1994) [Erratum-ibid. A **9**, 4353 (1994)] [arXiv:hep-th/9306002].
- [21] V. A. Fateev, Phys. Lett. B **357**, 397 (1995).
- [22] I. Affleck and A. W. W. Ludwig, Phys. Rev. Lett. **67**, 161 (1991).
- [23] A.I. B. Zamolodchikov, “Generalized Mathie Equation and Liouville TBA,” in “Quantum Field Theories in Two Dimensions: Collected works of Alexei Zamolodchikov,” vol.2, by A. Belavin, Ya. Pugai and A. Zamolodchikov (eds), World Scientific (2012).
- [24] P. Dorey, C. Dunning and R. Tateo, J. Phys. A **40**, R205 (2007) [arXiv:hep-th/0703066].
- [25] P. Dorey and R. Tateo, J. Phys. A **32**, L419 (1999) [arXiv:hep-th/9812211].
- [26] L.D. Landau and E.M. Lifshitz, Quantum Mechanics: Non-Relativistic Theory, vol.3, Third Edition Pergamon Press, Oxford (1997).